1140

NEANDC(J)-75/U
INDC(JAP)-62/U

NOT FOR PUBLICATION

PROGRESS REPORT

(July 1980 to June 1981 inclusive)

September 1981

Editor
S. Kikuchi
Japanese Nuclear Data Committee

Japan Atomic Energy Research Institute
Tokai Research Establishment
Tokai-mura, Ibaraki-ken, Japan

NEANDC(J)-75/U
INDC(JAP)-62/U

NOT FOR PUBLICATION

PROGRESS REPORT

(July 1980 to June 1981 inclusive)

September 1981

Editor

S. Kikuchi

Japanese Nuclear Data Committee

Japan Atomic Energy Research Institute

Tokai Research Establishment

Tokai-mura, Ibaraki-ken, Japan

Editor's Note

This is a collection of reports which have been submitted to the Japanese Nuclear Data Committee at the committee's request. The request was addressed to the following individuals who might represent or be in touch with groups doing researches related to the nuclear data of interest to the development of the nuclear energy program.

Although the editor tried not to miss any appropriate addressees, there may have been some oversight. Meanwhile, contribution of a report rested with discretion of its author. The coverage of this document, therefore, may not be uniform over the related field of research.

In this progress report, each individual report is generally reproduced as it was received by the JNDC Secretariat, and editor also let pass some simple obvious errors in the manuscripts if any.

This edition covers a period of July 1, 1980 to June 30, 1981. The information herein contained is of a nature of "Private Communication". Data contained in this report should not be quoted without the author's permission.

TABLE OF CONTENTS

CONTENTS OF JAPANESE PROGRESS REPORT NEANDC(J)-75U (SEPT.1981) PAGE 1

ELEMENT S	A	QUANTITY	ENERGY MIN	MAX	LAB	TYPE	DOCUMENTATION REF	VOL	PAGE	DATE	COMMENTS
LI		N EMISSION	14+7		OSA	EXPT-PROG	NEANDC-J75U		50	AUG 19	TAKAHASHI+.TOF.DOUBLE DIFF SIG.FIG
LI	6	N, DEUTERON	14+7		YOK	THEO-PROG	NEANDC-J75U		56	AUG 19	SHIBATA+.FINITE RANGE DWBA ANAL.FIG
LI	6	N, TRITON	14+7		YOK	THEO-PROG	NEANDC-J75U		56	AUG 19	SHIBATA+.FINITE RANGE DWBA ANAL.FIG
C	12	DIFF ELASTIC	14+7		OSA	EXPT-PROG	NEANDC-J75U		50	AUG 19	TAKAHASHI+.TOF.18 TO 144 DEG IN TBL
C	12	DIFF INELAST	14+7		OSA	EXPT-PROG	NEANDC-J75U		50	AUG 19	TAKAHASHI+.TOF.SIGS OF 3 LVLS IN TBL
C	12	N EMISSION	14+7		OSA	EXPT-PROG	NEANDC-J75U		50	AUG 19	TAKAHASHI+.TOF.DOUBLE DIFF SIG.FIG
C	12	N EMISSION	15+7		TOH	EXPT-PROG	NEANDC-J75U		61	AUG 19	IWASAKI+.TOF.DOUBLE DIFF SIG.NDG
MG	24	N, PROTON	FISS		KTO	EXPT-PROG	NEANDC-J75U		30	AUG 19	KOBAYASHI+.SUBMITTED TO NST.
MG	27	N, GAMMA	PILE		JAE	EXPT-PROG	NEANDC-J75U		17	AUG 19	SEKINE+.PUBLISHED IN JIN 41 1457
AL	27	N, 2N	FISS		JAE	EXPT-PROG	NEANDC-J75U		5	AUG 19	SATO+.ACTIV.SIG=4 MUB.
AL	27	N EMISSION	14+7		OSA	EXPT-PROG	NEANDC-J75U		50	AUG 19	TAKAHASHI+.TOF.DOUBLE DIFF SIG.FIG
AL	27	N EMISSION	NDG		TOH	EXPT-PROG	NEANDC-J75U		61	AUG 19	IWASAKI+.TOF.DOUBLE DIFF SIG.NDG
AL	27	N, PROTON	NDG		KTO	EXPT-PROG	NEANDC-J75U			AUG 19	KOBAYASHI+.SUBMITTED TO NST.
AL	27	N, ALPHA	NDG		KTO	EXPT-PROG	NEANDC-J75U			AUG 19	KOBAYASHI+.SUBMITTED TO NST.
AL	28	N, PROTON	FISS		JAE	EXPT-PROG	NEANDC-J75U		17	AUG 19	SEKINE+.SIG LT 0.002
S	32	N, PROTON	NDG		KTO	EXPT-PROG	NEANDC-J75U			AUG 19	KOBAYASHI+.SUBMITTED TO NST.
TI		N EMISSION	NDG		TOH	EXPT-PROG	NEANDC-J75U		61	AUG 19	IWASAKI+.TOF.DOUBLE DIFF SIG.NDG
V	51	N, PROTON	NDG		KTO	EXPT-PROG	NEANDC-J75U			AUG 19	KOBAYASHI+.SUBMITTED TO NST.
FE	54	N, PROTON	NDG		KTO	EXPT-PROG	NEANDC-J75U			AUG 19	KOBAYASHI+.SUBMITTED TO NST.
FE	56	N, PROTON	NDG		KTO	EXPT-PROG	NEANDC-J75U			AUG 19	KOBAYASHI+.SUBMITTED TO NST.

ELEMENT S	A	QUANTITY	ENERGY MIN	MAX	LAB	TYPE	DOCUMENTATION REF	VOL	PAGE	DATE	COMMENTS
FE	56	RESON PARAMS	50+3	80+4	TIT	EXPT-PROG	NEANDC-J75U		70	AUG 19	KOMANO+.PARTIAL RAD WIDTH.TABLE
CO	59	N, 2N	FISS		JAE	EXPT-PROG	NEANDC-J75U		16	AUG 19	SEKINE+.PUBLISHED IN JIN 43 1997
CO	69	N, ALPHA	NDG		KTO	EXPT-PROG	NEANDC-J75U			AUG 19	KOBAYASHI+.SUBMITTED TO NST.
NI	58	N, 2N	FISS		JAE	EXPT-PROG	NEANDC-J75U		16	AUG 19	SEKINE+.PUBLISHED IN JIN 43 1997
NI	58	N, 2N	FISS		JAE	EXPT-PROG	NEANDC-J75U		17	AUG 19	SEKINE+.PUBLISHED IN JIN 40 1977
NI	58	N, PROTON	NDG		KTO	EXPT-PROG	NEANDC-J75U			AUG 19	KOBAYASHI+.SUBMITTED TO NST.
NI	65	N, GAMMA	25-2		JAE	EXPT-PROG	NEANDC-J75U		17	AUG 19	SEKINE+.PUBLISHED IN JIN 40 1977
NI	65	RES INT CAP	50-1		JAE	EXPT-PROG	NEANDC-J75U		17	AUG 19	SEKINE+.PUBLISHED IN JIN 40 1977
ZN	64	N, PROTON	NDG		KTO	EXPT-PROG	NEANDC-J75U			AUG 19	KOBAYASHI+.SUBMITTED TO NST.
GE	70	N, 2N	FISS		JAE	EXPT-PROG	NEANDC-J75U		16	AUG 19	SEKINE+.PUBLISHED IN JIN 43 1997
RB	85	N, GAMMA	NDG		JAE	EXPT-PROG	NEANDC-J75U		4	AUG 19	OHKUBO+.LINAC TOF,LIQUID SC-T.NDG.
RB	85	RESON PARAMS	10+2	17+4	JAE	EXPT-PROG	NEANDC-J75U		4	AUG 19	OHKUBO+.LINAC TOF.100 RES LVLS.
RB	85	STRNTH FNCTN	10+2	17+4	JAE	EXPT-PROG	NEANDC-J75U		4	AUG 19	OHKUBO+.LINAC TOF.SO=0.93+-0.14 E-4.
RB	87	RESON PARAMS	20+2	10+5	JAE	EXPT-PROG	NEANDC-J75U		4	AUG 19	OHKUBO+.LINAC TOF.42 RES LVLS.
SR		TOTAL	10+4	15+7	NIG	EVAL-PROG	NEANDC-J75U		9	AUG 19	IIJIMA+.OPT MDL FITT.FIGS GIVEN.
SR	90	N, 2N	FISS		JAE	EXPT-PROG	NEANDC-J75U		16	AUG 19	SEKINE+.PUBLISHED IN JIN 43 1997
Y	89	TOTAL	10+4	15+7	NIG	EVAL-PROG	NEANDC-J75U		9	AUG 19	IIJIMA+.OPT MDL FITT.FIGS GIVEN.
ZR		TOTAL	10+4	15+7	NIG	EVAL-PROG	NEANDC-J75U		9	AUG 19	IIJIMA+.OPT MDL FITT.FIGS GIVEN.
NB	93	TOTAL	10+4	15+7	NIG	EVAL-PROG	NEANDC-J75U		9	AUG 19	IIJIMA+.OPT MDL FITT.FIGS GIVEN.
NB	93	N, GAMMA	32+3	80+4	TIT	EXPT-PROG	NEANDC-J75U		76	AUG 19	YAMAMURO+.PUBLISHED IN NST 17 582

ELEMENT S	A	QUANTITY	ENERGY MIN	MAX	LAB	TYPE	DOCUMENTATION REF	VOL	PAGE	DATE	COMMENTS
NB	94	N, GAMMA	PILE		JAE	EXPT-PROG	NEANDC-J75U		17	AUG 19	SEKINE+.PUBLISHED IN JIN 40 1973
MO		TOTAL	10+4	15+7	NIG	EVAL-PROG	NEANDC-J75U		9	AUG 19	IIJIMA+.OPT MDL FITT.FIGS GIVEN.
MO		N EMISSION	NDG		TOH	EXPT-PROG	NEANDC-J75U		61	AUG 19	IWASAKI+.TOF.DOUBLE DIFF SIG.NDG
TC	99	TOTAL	10+4	15+7	NIG	EVAL-PROG	NEANDC-J75U		9	AUG 19	IIJIMA+.OPT MDL FITT.FIGS GIVEN.
RU		TOTAL	10+4	15+7	NIG	EVAL-PROG	NEANDC-J75U		9	AUG 19	IIJIMA+.OPT MDL FITT.FIGS GIVEN.
PD		TOTAL	10+4	15+7	NIG	EVAL-PROG	NEANDC-J75U		9	AUG 19	IIJIMA+.OPT MDL FITT.FIGS GIVEN.
AG		TOTAL	10+4	15+7	NIG	EVAL-PROG	NEANDC-J75U		9	AUG 19	IIJIMA+.OPT MDL FITT.FIGS GIVEN.
AG	107	N, GAMMA	33+3	70+5	JAE	EXPT-PROG	NEANDC-J75U		3	AUG 19	SUGIMOTO+.LINAC TOF,LIQUID SC-T.NDG.
AG	107	RESON PARAMS	NDG		JAE	EXPT-PROG	NEANDC-J75U		3	AUG 19	MIZUMOTO+.LINAC TOF,NDG.
AG	109	N, GAMMA	33+3	70+5	JAE	EXPT-PROG	NEANDC-J75U		3	AUG 19	SUGIMOTO+.LINAC TOF,LIQUID SC-T.NDG.
AG	109	N, GAMMA	33+3	70+5	JAE	EXPT-PROG	NEANDC-J75U		3	AUG 19	SUGIMOTO+.LINAC TOF,LIQUID SC-T.NDG.
AG	109	RESON PARAMS	NDG		JAE	EXPT-PROG	NEANDC-J75U		3	AUG 19	MIZUMOTO+.LINAC TOF,NDG.
CD		TOTAL	10+4	15+7	NIG	EVAL-PROG	NEANDC-J75U		9	AUG 19	IIJIMA+.OPT MDL FITT.FIGS GIVEN.
IN		TOTAL	10+4	15+7	NIG	EVAL-PROG	NEANDC-J75U		9	AUG 19	IIJIMA+.OPT MDL FITT.FIGS GIVEN.
IN	113	TOT INELAST	NDG		KTO	EXPT-PROG	NEANDC-J75U			AUG 19	KOBAYASHI+.SUBMITTED TO NST.
IN	113	TOT INELAST	NDG		KTO	EXPT-PROG	NEANDC-J75U			AUG 19	KOBAYASHI+.SUBMITTED TO NST.
SN		TOTAL	10+4	15+7	NIG	EVAL-PROG	NEANDC-J75U		9	AUG 19	IIJIMA+.OPT MDL FITT.FIGS GIVEN.
SN		SPECT N,GAMM	40+5		TIT	EXPT-PROG	NEANDC-J75U		72	AUG 19	IGASHIRA+.NAI(TL).FJG
SB		TOTAL	10+4	15+7	NIG	EVAL-PROG	NEANDC-J75U		9	AUG 19	IIJIMA+.OPT MDL FITT.FIGS GIVEN.
TE		TOTAL	10+4	15+7	NIG	EVAL-PROG	NEANDC-J75U		9	AUG 19	IIJIMA+.OPT MDL FITT.FIGS GIVEN.

ELEMENT S	A	QUANTITY	ENERGY MIN	MAX	LAB	TYPE	DOCUMENTATION REF	VOL	PAGE	DATE	COMMENTS
I	127	TOTAL	10+4	15+7	NIG	EVAL-PROG	NEANDC-J75U		9	AUG 19	IIJIMA+.OPT MDL FITT.FIGS GIVEN.
I	127	N, GAMMA	32+3	80+4	TIT	EXPT-PROG	NEANDC-J75U		76	AUG 19	YAMAMURO+.PUBLISHED IN NST 17 582
XE		TOTAL	10+4	15+7	NIG	EVAL-PROG	NEANDC-J75U		9	AUG 19	IIJIMA+.OPT MDL FITT.FIGS GIVEN.
CS	133	TOTAL	10+4	15+7	NIG	EVAL-PROG	NEANDC-J75U		9	AUG 19	IIJIMA+.OPT MDL FITT.FIGS GIVEN.
CS	133	SPECT N,GAMM	15+3	75+4	TIT	EXPT-PROG	NEANDC-J75U		74	AUG 19	SHIRAYANAGI+.C6D6 LIQUID SCIN.FIG.
BA		TOTAL	10+4	15+7	NIG	EVAL-PROG	NEANDC-J75U		9	AUG 19	IIJIMA+.OPT MDL FITT.FIGS GIVEN.
LA	139	TOTAL	10+4	15+7	NIG	EVAL-PROG	NEANDC-J75U		9	AUG 19	IIJIMA+.OPT MDL FITT.FIGS GIVEN.
LA	139	N, GAMMA		25+3	JAE	EXPT-PROG	NEANDC-J75U		2	AUG 19	NAKAJIMA+.SUBMITTED TO NST.
LA	139	RESON PARAMS		25+3	JAE	EXPT-PROG	NEANDC-J75U		2	AUG 19	NAKAJIMA+.SUBMITTED TO NST.
CE		TOTAL	10+4	15+7	NIG	EVAL-PROG	NEANDC-J75U		9	AUG 19	IIJIMA+.OPT MDL FITT.FIGS GIVEN.
PR	141	TOTAL	10+4	15+7	NIG	EVAL-PROG	NEANDC-J75U		9	AUG 19	IIJIMA+.OPT MDL FITT.FIGS GIVEN.
ND		TOTAL	10+4	15+7	NIG	EVAL-PROG	NEANDC-J75U		9	AUG 19	IIJIMA+.OPT MDL FITT.FIGS GIVEN.
PM	147	TOTAL	10+4	15+7	NIG	EVAL-PROG	NEANDC-J75U		9	AUG 19	IIJIMA+.OPT MDL FITT.FIGS GIVEN.
SM		TOTAL	10+4	15+7	NIG	EVAL-PROG	NEANDC-J75U		9	AUG 19	IIJIMA+.OPT MDL FITT.FIGS GIVEN.
SM	147	N, GAMMA	33+3	30+5	JAE	EXPT-PROG	NEANDC-J75U		1	AUG 19	MIZUMOTO.PUBLISHED IN NP/A357 90.
SM	147	RESON PARAMS		20+3	JAE	EXPT-PROG	NEANDC-J75U		1	AUG 19	MIZUMOTO.PUBLISHED IN NP/A357 90.
SM	147	STRNTH FNCTN		20+3	JAE	EXPT-PROG	NEANDC-J75U		1	AUG 19	MIZUMOTO.PUBLISHED IN NP/A357 90.
SM	149	N, GAMMA	33+3	30+5	JAE	EXPT-PROG	NEANDC-J75U		1	AUG 19	MIZUMOTO.PUBLISHED IN NP/A357 90.
SM	149	RESON PARAMS		52+2	JAE	EXPT-PROG	NEANDC-J75U		1	AUG 19	MIZUMOTO.PUBLISHED IN NP/A357 90.
SM	149	STRNTH FNCTN		52+2	JAE	EXPT-PROG	NEANDC-J75U		1	AUG 19	MIZUMOTO.PUBLISHED IN NP/A357 90.

ELEMENT S	A	QUANTITY	ENERGY MIN	MAX	LAB	TYPE	DOCUMENTATION REF VOL	PAGE	DATE	COMMENTS
EU		TOTAL	10+4	15+7	NIG	EVAL-PROG	NEANDC-J75U	9	AUG 19	IIJIMA+.OPT MDL FITT.FIGS GIVEN.
GD		TOTAL	10+4	15+7	NIG	EVAL-PROG	NEANDC-J75U	9	AUG 19	IIJIMA+.OPT MDL FITT.FIGS GIVEN.
DY	165	N, GAMMA	PILE		JAE	EXPT-PROG	NEANDC-J75U	17	AUG 19	SEKINE+.G AND M TARGETS.SIGS GIVEN.
HO	165	N, GAMMA	32+3	80+4	TIT	EXPT-PROG	NEANDC-J75U	76	AUG 19	YAMAMURO+.PUBLISHED IN NST 17 582
TA	181	N, GAMMA	32+3	80+4	TIT	EXPT-PROG	NEANDC-J75U	76	AUG 19	YAMAMURO+.PUBLISHED IN NST 17 582
AU	197	N, 2N	NDG		KTO	EXPT-PROG	NEANDC-J75U		AUG 19	KOBAYASHI+.SUBMITTED TO NST.
HG	199	TOT INELAST	78+5	63+6	JAE	EXPT-PROG	NEANDC-J75U	14	AUG 19	SAKURAI+.TO ISOMER.SUBMITTED TO NST
TL	203	N, 2N	FISS		JAE	EXPT-PROG	NEANDC-J75U	16	AUG 19	SEKINE+.PUBLISHED IN JIN 43 1997
PB		N EMISSION	14+7		OSA	EXPT-PROG	NEANDC-J75U	50	AUG 19	TAKAHASHI+.TOF.DOUBLE DIFF SIG.FIG
TH	228	EVALUATION	10-5	20+7	KYU	EVAL-PROG	NEANDC-J75U	41	AUG 19	OHSAWA+.SEE MEMO OF FAC ENG 40 149.
TH	230	EVALUATION	10-5	20+7	KYU	EVAL-PROG	NEANDC-J75U	41	AUG 19	OHSAWA+.SEE MEMO OF FAC ENG 40 149.
TH	232	EVALUATION	10-5	20+7		EVAL-PROG	NEANDC-J75U	40	AUG 19	OHSAWA+.PUBLISHED IN NST 18 408
TH	232	TOTAL	50+4	10+7	TOH	EXPT-PROG	NEANDC-J75U	66	AUG 19	IWASAKI+.LI THICK TARGET,TOF.NDG
TH	232	TOTAL	-3	20+1	KTO	EXPT-PROG	NEANDC-J75U	25	AUG 19	KOBAYASHI+.LINAC TOF.FIG GIVEN.
TH	232	DIFF ELASTIC	55+5	57+6	TOH	EXPT-PROG	NEANDC-J75U	68	AUG 19	IWASAKI+.TOF.NDG.
TH	232	DIFF INELAST	55+5	57+6	TOH	EXPT-PROG	NEANDC-J75U	68	AUG 19	IWASAKI+.TOF.NDG.
TH	232	SPECT FISS N	16+6		TOH	EXPT-PROG	NEANDC-J75U	63	AUG 19	TAMURA+.TOF,MAXW-TEMP=1.37+-0.05 MEV
TH	233	EVALUATION	10-5	20+7	KYU	EVAL-PROG	NEANDC-J75U	41	AUG 19	OHSAWA+.SEE MEMO OF FAC ENG 40 149.
TH	234	EVALUATION	10-5	20+7	KYU	EVAL-PROG	NEANDC-J75U	41	AUG 19	OHSAWA+.SEE MEMO OF FAC ENG 40 149.
U	235	FISSION	10+5	10+7	KYU	EVAL-PROG	NEANDC-J75U	46	AUG 19	UENOHARA+.SIMULTANEOUS EVAL.FIG

ELEMENT S	A	QUANTITY	ENERGY MIN	MAX	LAB	TYPE	DOCUMENTATION REF	VOL	PAGE	DATE	COMMENTS
U	235	FISS PROD GS	NDG			EXPT-PROG	NEANDC-J75U		49	AUG 19	YAMAMOTO+.LA143,PR147.JIN 43 855
U	235	FISS PROD GS	MAXW		NIG	EVAL-PROG	NEANDC-J75U		12	AUG 19	YOSHIDA+.PUBLISHED IN NST 18 393
U	235	FISS PROD GS	NDG		NAG	EXPT-PROG	NEANDC-J75U		48	AUG 19	YAMAMOTO+.CE145,146 LIFE.JIN 42 1539
U	235	FISS PROD BS	MAXW		NIG	EVAL-PROG	NEANDC-J75U		12	AUG 19	YOSHIDA+.PUBLISHED IN NST 18 393
U	238	TOTAL	20+4	10+6	JAE	EXPT-PROG	NEANDC-J75U		45	AUG 19	TSUBONE+.LINAC TOF,FE-FILTER.FIG
U	238	N, GAMMA	32+3	80+4	TIT	EXPT-PROG	NEANDC-J75U		76	AUG 19	YAMAMURO+.PUBLISHED IN NST 17 582
U	238	FISSION	TR	10+7	KYU	EVAL-PROG	NEANDC-J75U		46	AUG 19	UENOHARA+.SIMULTANEOUS EVAL.FIG
CM	243	EVALUATION	10-5	20+7	JAE	EVAL-PROG	NEANDC-J75U		7	AUG 19	NAKAGAWA+.PUBLISHED AS JAERI-M 9601.
MANY		N, PROTON	14+7			THEO-PROG	NEANDC-J75U		38	AUG 19	HYAKUTAKE+.PEEQ MDL ANAL.FIG GIVEN.
MANY		N, ALPHA	14+7		KYU	THEO-PROG	NEANDC-J75U		33	AUG 19	KUMABE.PREEQ MDL ANAL.FIG GIVEN.
MANY		N, ALPHA	14+7			THEO-PROG	NEANDC-J75U		38	AUG 19	HYAKUTAKE+.PEEQ MDL ANAL.FIG GIVEN.
MANY		FISSION	NDG		KYU	THEO-PROG	NEANDC-J75U		42	AUG 19	OHSAWA+.SEE MEMO OF FAC ENG 41 143

The content table in the CINDA format was compiled by the JNDC CINDA group;

S. Tanaka (JAERI), R. Nakasima (Hosei Univ.),
Y. Kawarasaki (JAERI), M. Sakamoto (JAERI),
M. Kawai (NAIG), Y. Kikuchi (JAERI).

I. JAPAN ATOMIC ENERGY RESEARCH INSTITUTE

A. Linac Laboratory, Division of Physics

I-A-1 Neutron Resonance Parameters and Radiative Capture Cross Sections of ^{147}Sm and ^{149}Sm.

M. Mizumoto

A paper on this subject has been published in Nuclear Physics A357 (1981) 90 - 108 with an abstract as follows:

Neutron capture and transmission measurements have been carried out on the separated isotopes of ^{147}Sm (98.34 %) and ^{149}Sm (97.72 %) at the 55 m time-of-flight station of the Japan Atomic Energy Research Institute electron linear accelerator. Resonance energies and neutron widths for a large number of resolved resonances were determined up to 2 keV for ^{147}Sm and 520 eV for ^{149}Sm. Radiation widths for 5 resonances in $^{147}Sm + n$ and 7 resonances in $^{149}Sm + n$ were derived. The s-wave strength functions, average level spacings and average radiation widths were obtained to be: $10^4 S_0 = 4.8 \pm 0.5$, $\bar{D} = 5.7 \pm 0.5$ eV and $\bar{\Gamma}_\gamma = 69 \pm 2$ meV for ^{147}Sm; and $10^4 S_0 = 4.6 \pm 0.6$, $\bar{D} = 2.2 \pm 0.2$ eV and $\bar{\Gamma}_\gamma = 62 \pm 2$ meV for ^{149}Sm. The average capture cross sections were deduced from 3.3 to 300 keV with an estimated accuracy of 5 to 15 %. The measured capture cross sections for ^{149}Sm are largely different from the evaluated data, which are obtained based on the statistical model calculation. Possible reasons for this disagreement are discussed.

I-A-2 Neutron Resonances in ^{139}La below 2.5 keV

Y. Nakajima, N. Ohnishi*,+, Y. Kanda*
M. Mizumoto, Y. Kawarasaki, Y. Furuta
and A. Asami*

A paper on this subject was submitted to Journal of Nuclear Science and Technology.

The radiative neutron capture cross section of ^{139}La has been measured below 2.5 keV using the Japan Atomic Energy Research Insititute linac neutron time-of-flight facility with a 50 m flight path. Individual resonances were analyzed with a Monte Carlo area analysis method[1)] to obtain the capture widths of the resonances below 2.5 keV. The capture widths Γ_γ of five resonances and the capture areas $g\Gamma_n\Gamma_\gamma/\Gamma$ of twenty resonances were newly obtained. The average capture cross section of ^{139}La can be fitted by the statistical calculation even in the intermediate structure region.

1) F. H. Fröhner, GA-6906(1966)

---

* Graduate School of Engineering Sciences, Kyushu University
+ Present address: Shikoku Electric Co., Inc.
++ Present address: National Laboratory for High Energy Physics

I-A-3 Average Neutron Capture Cross Sections of Silver Isotopes in the keV region.

M. Sugimoto, M. Mizumoto, Y. Nakajima, Y. Kawarasaki,

Y. Furuta and A. Asami*

The neutron capture cross sections of silver isotopes have been measured by using a large liquid scintillation detector at a 55 m station. Average cross section were deduced from 3.3 to 700 keV with an accuracy of 5 to 10 %. Our results of natural and ^{107}Ag samples are in good agreement with earlier data, while our results of ^{109}Ag lie between previous two data; 30 % higher than those by Weston et al.[1] and 35 % lower than those by Kononov et al.[2]

References:

1) L.W. Weston et al., Ann. of Phys. 10 (1960) 477.

2) V.N. Kononov et al., Proc. of Conf. on Nuclear Data for Reactors, Paris, 1966.

---

*Present Address: National Laboratory for High Energy Physics.

I-A-4 Resonance Parameters of ^{107}Ag and ^{109}Ag.

M. Mizumoto, M. Sugimoto, M. Ohkubo, Y. Nakajima,

Y. Kawarasaki and Y. Furuta

Transmissions of ^{107}Ag and ^{109}Ag were measured at 55 m and 190 m time-of-flight stationsof the JAERI linac facility. The transmission data are analyzed with a multi-level Breit-Wigner formula to obtain neutron widths of resonances in combination with capture data taken with a large liquid scintillation detector.

I-A-5

Neutron Resonance Parameters of ^{85}Rb and ^{87}Rb

M.OHKUBO, M.MIZUMOTO and Y.KAWARASAKI

Neutron transmission measurements on ^{85}Rb and ^{87}Rb were carried out at 47-m station of the JAERI linac TOF spectrometer with the maximum resolution of ~1 ns/m. Separated isotope samples(~98% enriched, chemical form RbCl) were used. For ^{85}Rb 100 levels are observed in 0.1~17 keV, and for ^{87}Rb 42 levels in 0.2~100 keV energy region. In comparison with the previous data[1), many resonance levels are newly observed. Resonance analyses were made on the transmission data, and obtained $g\Gamma_n^0$ values for 100 levels of ^{85}Rb in 0.1~17 keV region, and for 16 levels of ^{87}Rb in 0.2~23 keV region. s-wave strength function of ^{85}Rb is obtained to be $S_0=(0.93 \pm 0.14)10^{-4}$ in the measured region. Capture cross section measurements on ^{85}Rb were made by the liquid scintillator tank, and the data analyses are in progress.

1) Grebenyuk et al. JINR-P3-4357(1969)

B. Nuclear Chemistry Laboratory

Division of Chemistry

I-B-1 $^{27}Al(n.2n)^{26}Al$ Cross Section

T. Sato and T. Suzuki

The cross section of $^{27}Al(n,2n)^{26}Al$ for fission spectrum neutrons was determined to be 4μb by radiochemical techniques. An aluminum specimen was taken out from side plate of spent fuel elements from the Japan Research Reactor-2 in JAERI. After dissolving the specimen, aluminum, iron and manganese were separated by anion exchange with hydrochloric acid media and further purified by coprecipitation techniques. The amount of aluminum was weighed in a form of Al_2O_3 and that of iron in a form of ferric oxinate. Radioactivity of ^{26}Al in the aluminum separated was identified by its characteristic γ ray at 1809keV and determined to be 0.12 ± 0.016 dps/gAl with a Ge(Li) detector of which efficiency calibration was made by using LMRI reference sources of ^{88}Y and ^{54}Mn. Radioactivity of ^{54}Mn separated was also measured with the detector and the neutron flux for the specimen was obtained by taking 83mb for the cross section of $^{54}Fe(n,p)^{54}Mn$.

I-B-2

Half-life of ^{242}Cm

S. Usuda and H. Umezawa

1) A paper on the subject was accepted for publication in the Journal of Inorganic and Nuclear Chemistry with an abstract as follows:

Pure ^{242}Cm was prepared and the decay of alpha activity had been followed over 18 months. The half-life of ^{242}Cm was determined to be $161.35 \pm 0.30 (3\sigma)$ day. That is significantly shorter than the other data which have appeared in literature.

2) In addition, spontaneous fission rate of ^{242}Cm has been measured by mica detector techniques and a tentative value, $6.87 \pm 0.17 \times 10^6$y, was obtained as the spontaneous fission half-life of ^{242}Cm.

C. Nuclear Data Center, Division of Physics and Working Groups of Japanese Nuclear Data Committee

I-C-1 Evaluation of Neutron Nuclear Data for ^{243}Cm

T. Nakagawa and S. Igarasi

A Paper on this subject was published as JAERI-M 9601 with the following abstract,

The neutron nuclear data of ^{243}Cm were evaluated in the neutron energy region from 10^{-5} eV to 20 MeV. The evaluated quantities are resonance parameters up to 26 eV, the total, fission, capture, elastic and inelastic scattering, (n,2n), (n,3n) and (n,4n) reaction cross sections, angular distributions of emitted neutrons and the number of neutrons per fission. The measured data are very scarce. The evaluation was made mainly on the basis of the optical and statistical model calculations. The present results are compiled in the ENDF/B format, and they will be stored in the second version of Japanese Evaluated Nuclear Data Library, JENDL-2.

Fig. 1 shows the evaluated cross sections above 1 keV.

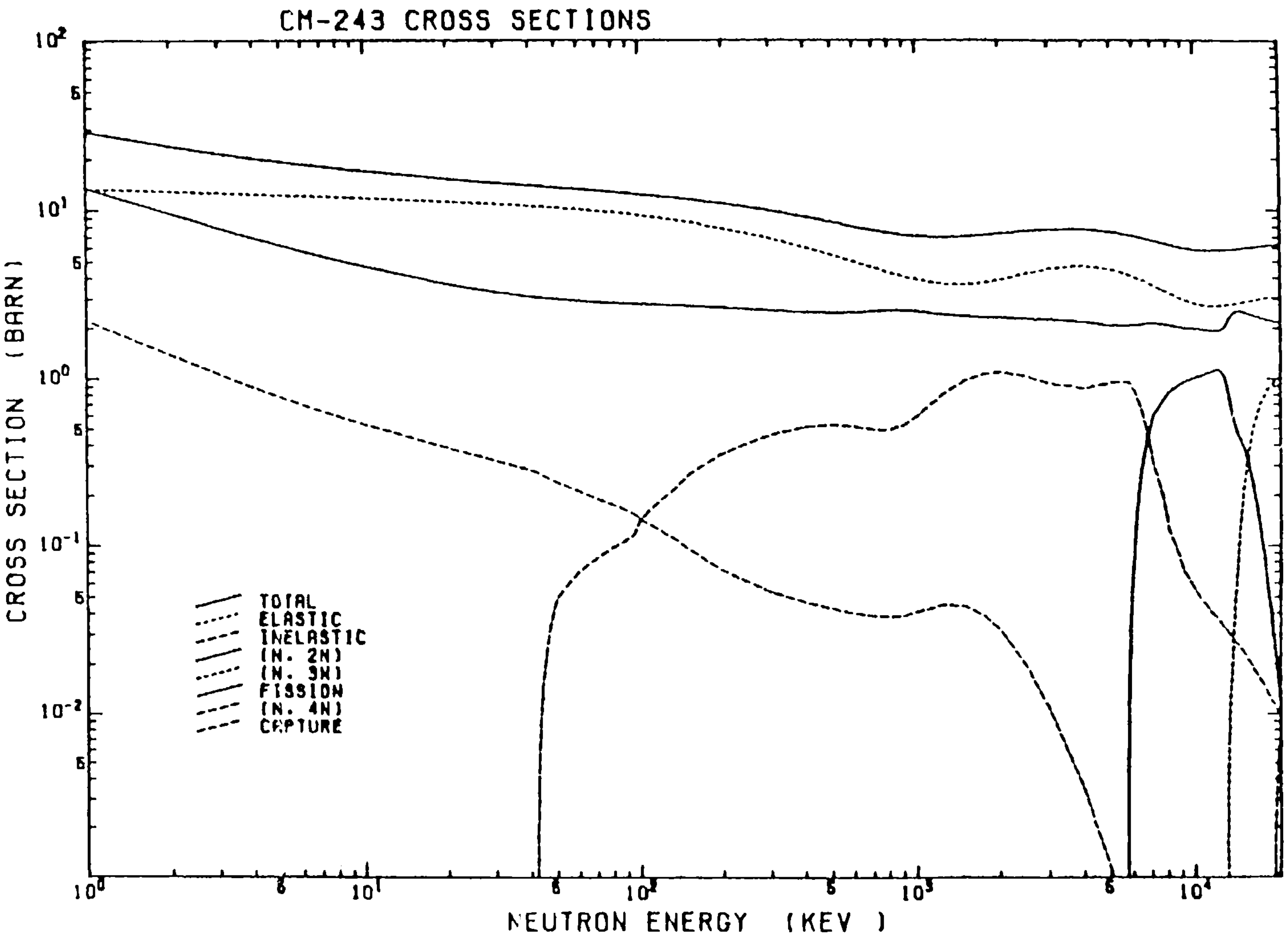

Fig. 1 Evaluated cross sections above 1 keV

I-C-2 Local Systematics of Fission Product Neutron Total Cross Sections and Determination of Optical Model Parameters

S. Iijima* and M. Kawai*

For JENDL-2 FP cross section evaluation, the spherical optical model parameters are being searched, taking account of the local systematics of experimental data for nearby nuclides. Fig. 1 (a)-(f) show that the measured total cross sections for natural elements in 10 keV -15 MeV exhibit the local systematics of intermediate scale, and can be grouped into several groups remarkably. Calculations by preliminary sets of OMP, each determined so as to fit the corresponding total cross section data for each group, are also depicted. (Small-scale local systematics such as known for Sn and Te isotopes is not taken into account.)

Following points were observed through the study.

(1) The experimental data of total cross sections are still lacking even for natural elements, especially in the energy range of 10 KeV - 1 MeV. More measurements on natural elements and separated isotopes will be very valuable.

(2) Neutron strength function data are often quite discrepant depending on the evaluators. We prefer to put more weight on total cross section data by the determination of OMP.

(3) In case of nuclides in 4S size resonance region (Nd, Pm, Sm, Eu), where SPR data vary rapidly as mass increases, the present results are not yet satisfactory.

Global systematic trend of the present OMP is being investigated.

---

* Nippon Atomic Industry Group Co. Ltd.

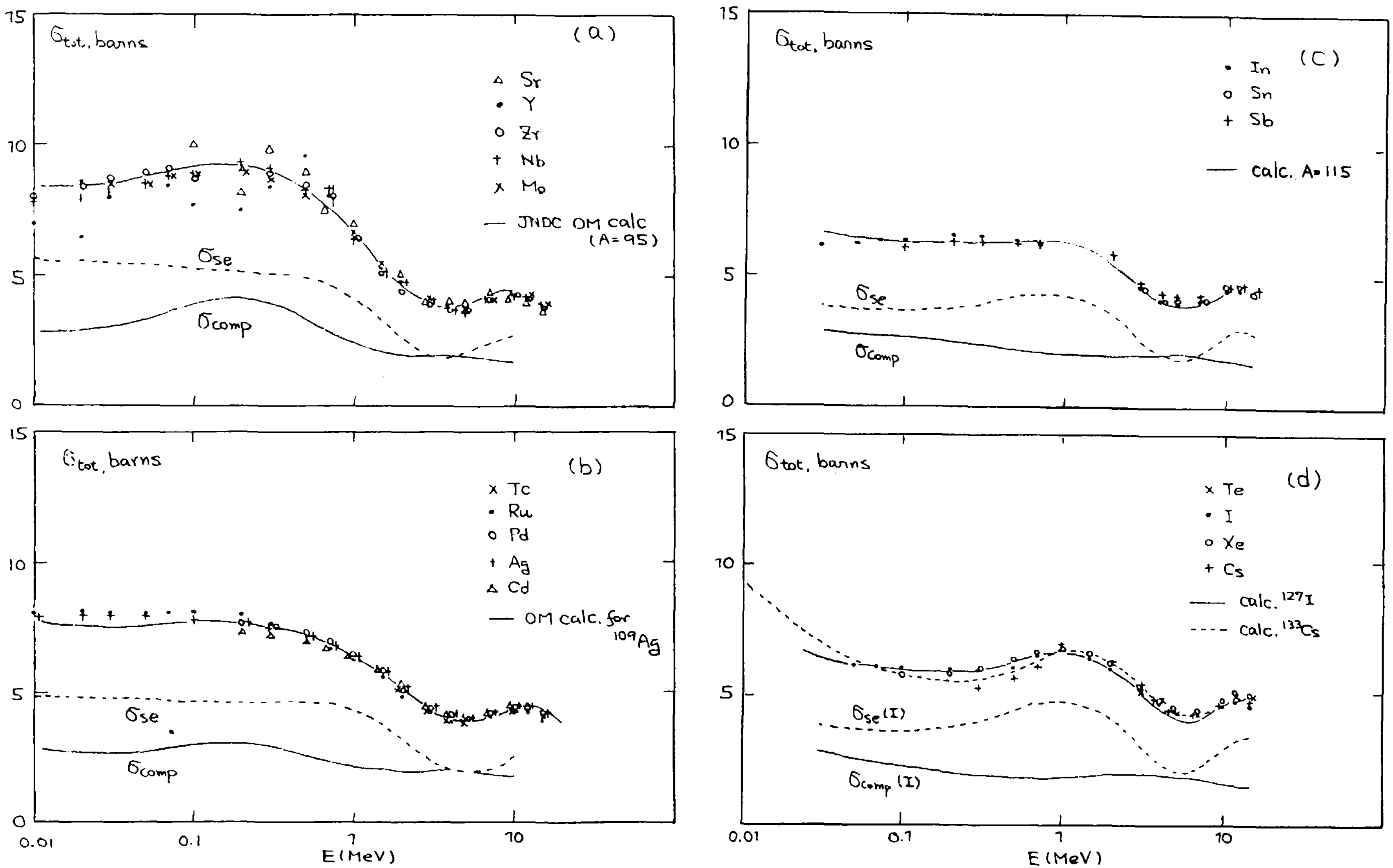

Fig. 1 Grouping of Measured Total Cross Sections for Natural Elements and Optical Model Fit

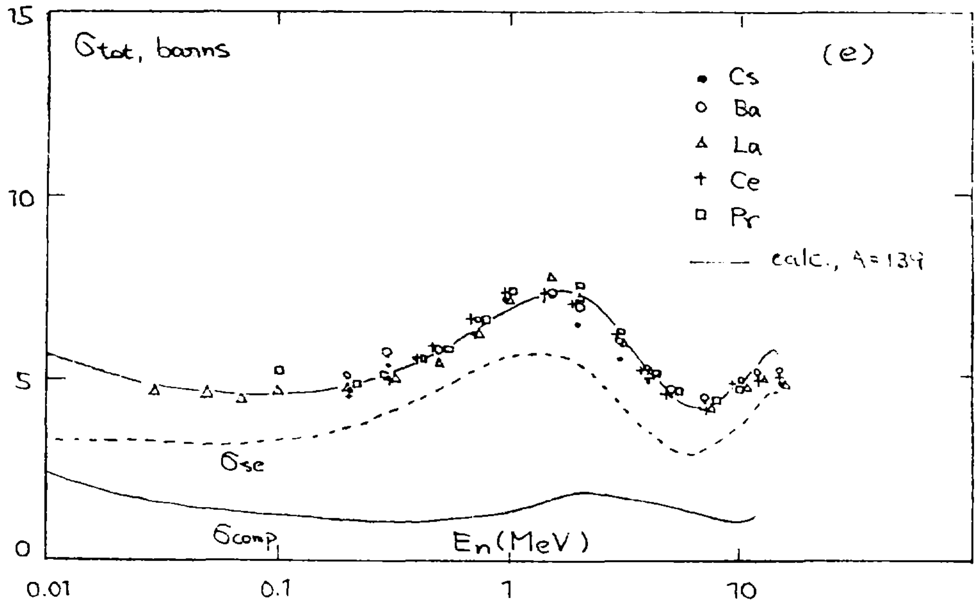

15
10
5
0
Gtot, barns
(e)
Cs
Ba
La
Ce
Pr
calc., A=134
Gse
Gcomp
En(MeV)
0.01
0.1
1
10

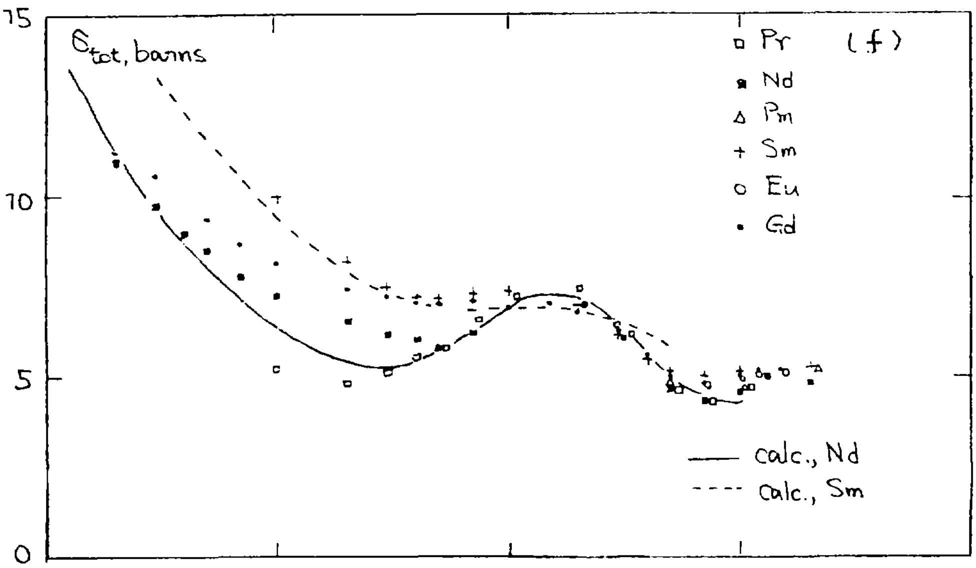

15
10
5
0
Gtot, barns
Pr
(f)
Nd
Pm
Sm
Eu
Gd
calc., Nd
calc., Sm

Fig. 1 (cont'd)

I-C-3

Decay Heat Calculations Based on Theoretical Estimation of Average Beta- and Gamma-Energies Released from Short-Lived Fission Products+

T. Yoshida* and R. Nakasima**

Fission product decay heat at short cooling times was studied on the basis of JNDC FP Decay Data File. It was shown that a full adoption of recent publication of decay schemes to derive average energies of β- and γ-rays ($\bar{E}_\beta$ and $\bar{E}_\gamma$) for short-lived FPs leads to a large underestimation of the γ-ray decay heat and to an overestimation of the β-ray decay heat. These results correspond to the curves (A) in Figs. 1 and 2. Theoretical values of $\bar{E}_\beta$ and $\bar{E}_\gamma$ were then introduced for short-lived FPs with high Q-values, which were obtained with a gross theory of beta-decay(1). As is shown in Figs. 1 and 2 with curves (B), it improved remarkably the agreement of calculation with experiment. It was concluded that a large part of decay schemes recently published for high Q-value nuclides are inappropriate to use in calculation of $\bar{E}_\beta$ and $\bar{E}_\gamma$, because they fail to reproduce the effect of β-strength at high excitations, which makes $\bar{E}_\beta$ small and $\bar{E}_\gamma$ large. The use of the gross theory introduces this effect correctly into the values of $\bar{E}_\beta$ and $\bar{E}_\gamma$ and, hence, leads to a quite good prediction of both β- and γ-decay heat. The final version of JNDC FP Decay Data File(2) adopts these theoretical values for high Q-value FPs.

(1) T. Yoshida, Nucl. Sci. Eng., 63, 376 (1977)

(2) T. Yamamoto et al., "JNDC FP Decay Data File," JAERI-M 9357 (1981)

+ This paper was published in Journal of Nuclear Science and Technology. 18 [6], pp. 393~407 (June, 1981)

* Nippon Atomic Industry Group Co. Ltd.

** Dept. of Physics, Hosei University

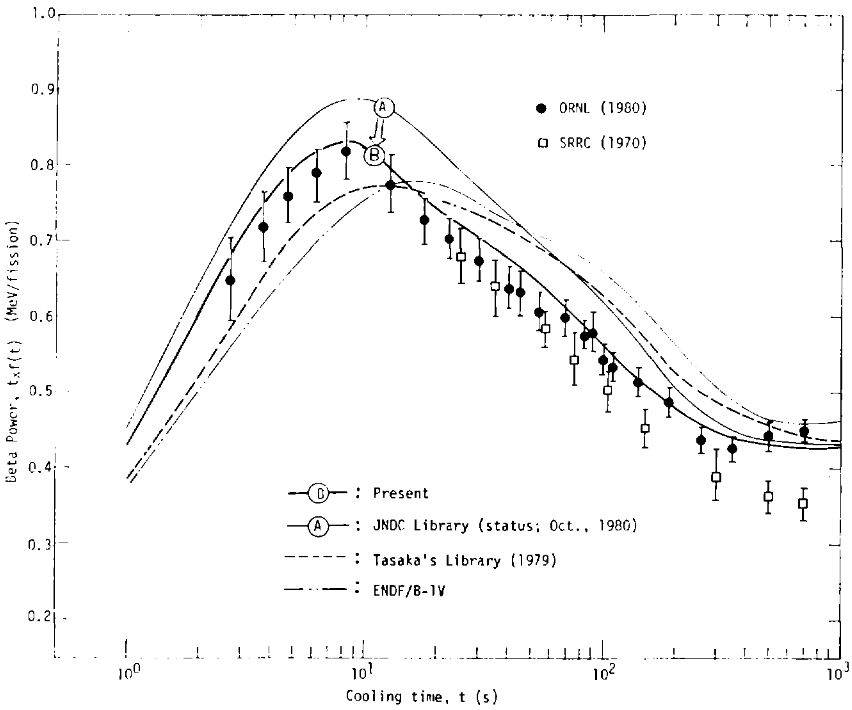

Fig. 1 Beta-ray decay heat after a burst neutron irradiation, U-235

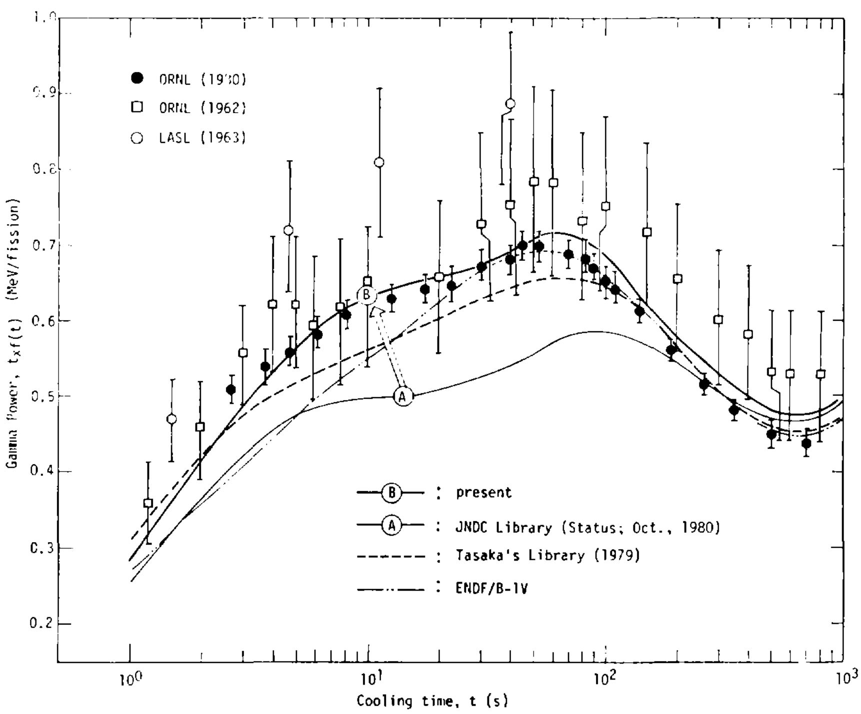

Fig. 2 Gamma-ray decay heat after a burst neutron irradiation, U-235

D. Project Engineering Section

Division of JMTR Project

I-D-1

Cross Section Measurement for the $^{199}Hg(n,n')^{199m}Hg$ Reaction from 0.78 to 6.3 MeV

K. Sakurai, H. Gotoh[+], S. Yamamoto[*], K. Kobayashi[*], and I. Kimura[*]

A paper on this subject will be submitted to the J. Nucl. Sci. and Technol.[1)]

Cross sections for the $^{199}Hg(n,n')^{199m}Hg$ reaction were measured at 10 energy points from 0.78 to 6.3 MeV by the activation method. Monoenergetic neutrons below 2 MeV were produced by the $^{7}Li(p,n)^{7}Be$ reaction and those above 2 MeV were produced by the $D(d,n)^{3}He$ reaction using a 5.5 MV Van de Graaff accelerator. The neutron flux was determined with a proton recoil telescope counter and indium foils. The measured cross sections were fitted with following expression,

$$\sigma(E) = 0.082 - \frac{0.67}{1 + (E/2.32)^{2.66}} + \frac{0.588}{1 + (E/11.44)^{10}}$$

where E is neutron energy in MeV and $\sigma(E)$ is neutron cross section in barn. The fission spectrum averaged cross section was calculated from the expression. The value is 247.5 mb for the Watt-type fission spectrum(ENDF/B-V)[2)], and it is about 12 % smaller than that measured recently[3)].

+ Reactor Instrumentation Laboratory
Division of Reactor Engineering

* Research Reactor Institute, Kyoto University

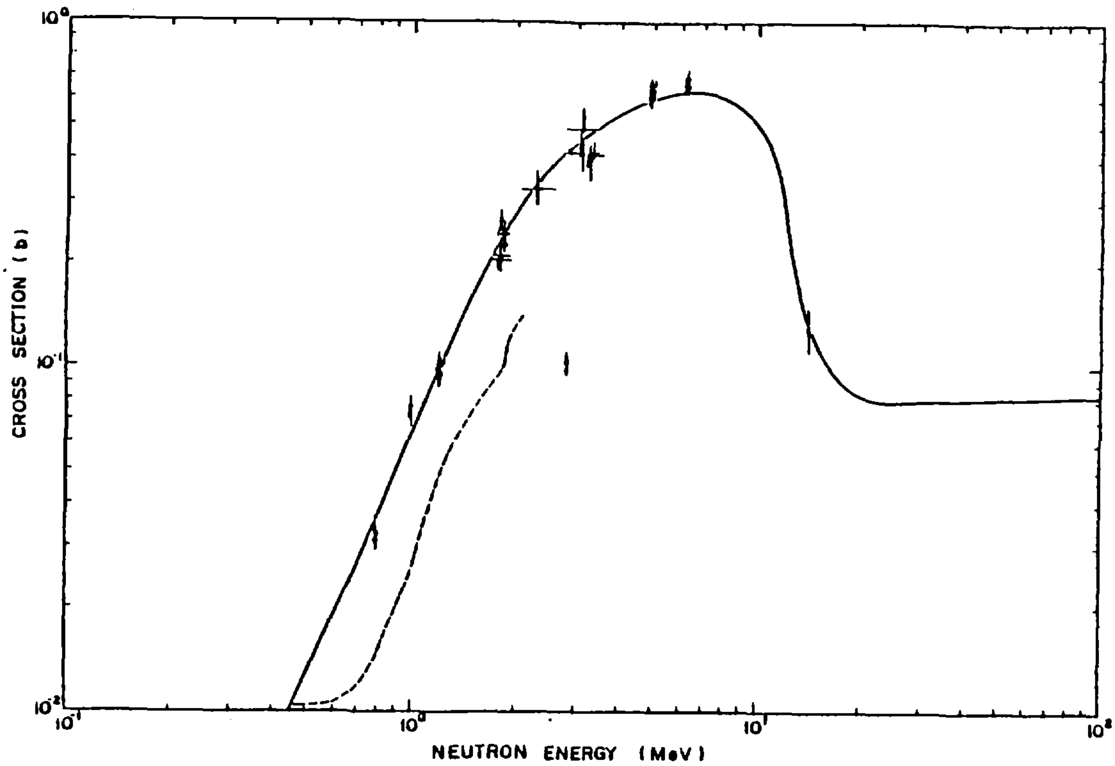

References:

1) K. Sakurai, H. Gotoh, S. Yamamoto, K. Kobayashi and I. Kimura, J. Nucl. Sci. and Technol.(to be submitted)

2) B. A. Magurno, EUR-6813, 2(1980)904

3) K. Kobayashi, S. Yamamoto and I. Kimura, Annu. Rep. Res. Reactor Inst., Kyoto Univ., 14(1981)1

E. Production Development Section

Division of Radioisotope Production

I-E-1 Cross Section of the (n,2n) Reaction of ^{59}Co, ^{58}Ni, ^{70}Ge, ^{90}Sr, and ^{203}Tl with Fission Neutrons

T. Sekine and H. Baba

A paper on this subject was published in J. inorg. nucl. Chem. 43 (1981) 1427.

The (n,2n) reaction cross sections for some target nuclides were determined by means of the activation method with fission neutrons. The values obtained ware 0.233 ± 0.017 mb for ^{59}Co, 4.06 ± 0.21 μb for ^{58}Ni, 0.723 ± 0.055 mb for ^{70}Ge, 0.1044 ± 0.046 mb for ^{90}Zr, and 3.93 ± 0.11 mb for ^{203}Tl. The cross-section value for ^{58}Ni is somewhat greater than that previously reported[1]. The change was caused because of the improvement of flux monitoring and activity measurement.

The obtained results are in good agreement with the values predicted by the authors[2]. The cross-section values calculated empirically or theoretically by several authors are compared with the observed values.

References:

1) T. Sekine and H. Baba, JAERI report JAERI-1266 (1980).

2) T. Sekine and H. Baba, J. inorg. nucl. Chem. 40 (1978) 1997.

I-E-2 A Study of Reactor-Neutron-Induced Reactions: Double Neutron Capture Process and the Systematics of the (n,2n) Reaction

T. Sekine and H. Baba

A paper on this subject was published in the Japan Atomic Energy Research Institute Report JAERI-1266 (1980).

Cross sections of the second neutron capture in the double-neutron-capture process were studied in the irradiation of ^{26}Mg, ^{64}Ni, ^{93}Nb, and ^{164}Dy with reactor neutrons. Weak radioactivities produced were determined with sufficient accuracy by taking advantage of chemical purification and the Ge(Li) γ-ray spectrometry. The neutron spectrum at the irradiating site was specified with Westcott's epithermal index determined by the use of the cadmium-ratio method.

Cross sections of $^{28}Al(n,p)^{28}Mg$ and $^{58}Ni(n,2n)^{57}Ni$ reactions with fission neutrons were also measured. A simple formula was proposed for the systematics of (n,2n) reaction cross sections, which enabled prediction of the cross section more accurately than the previously proposed formulae.

The cross-section values obtained are summarized in Table 1.

Table 1. Cross sections obtained in a study of reactor-neutron-induced reactions.

Reaction	Cross section(b)*	Westcott's index
$^{27}Mg(n,\gamma)^{28}Mg$	$\hat{\sigma} = 0.07 \pm 0.02$	0.017–0.075
$^{65}Ni(n,\gamma)^{66}Ni$	$\sigma_0 = 20.4 \pm 2.4$ $\underline{I} < 60$	
$^{94}Nb(n,\gamma)^{95m}Nb$	$\hat{\sigma} = 0.61 \pm 0.03$	0.022
$^{94}Nb(n,\gamma)^{95g}Nb$	$\hat{\sigma} = 14.6 \pm 0.3$	0.022
$^{94}Nb(n,\gamma)^{95m+g}Nb$	$\hat{\sigma} = 15.2 \pm 0.3$	0.022
$^{165m}Dy(n,\gamma)^{166}Dy$	$\hat{\sigma} = 2000 \pm 600$	0.017
$^{165g}Dy(n,\gamma)^{166}Dy$	$\hat{\sigma} = 3530 \pm 330$	0.017
$^{58}Ni(n,2n)^{57}Ni$	$\sigma_f = (3.8 \pm 0.5)\times 10^{-6}$	
$^{28}Al(n,p)^{28}Mg$	$\sigma_f < 0.002$	

*) $\hat{\sigma}$ is the effective cross section, σ_0 the cross section for 2200 $m \cdot sec^{-1}$ neutrons, $\underline{I}$ the resonance integral, and σ_f the fission-neutron-averaged cross section.

I-E-3 Half-life of ^{237}Pu

H. Baba, T. Suzuki, and K. Hata

A paper on this subject was published in J. inorg. nucl. Chem. 43 (1981) 1059.

The half-life of ^{237}Pu was determined by periodic measurement of the low-energy photon spectrum with a surface-barrier-type solid state detector for low-energy photon spectrometry. The measurement was repeated 43 times for about 600 days by observing the variation of the detection efficiency with an ^{241}Am reference source. The shaping time of the electronic circuit was set to 2 μsec and the total count rate was as low as 600 cps at the beginning of the measurement, so that the distortion of the obtained spectrum due to the pile-up effect was negligible. The length of the counting time was initially 50–60 ksec but extended to 240–400 ksec in the last stage of the measurement.

The ^{237}Pu sample was prepared by the $^{238}U(^{3}He,4n)^{237}Pu$ reaction using the cyclotron of the Institute of Physical and Chemical Research. The details of the experimental procedure are described elsewhere[1]. The source for the spectrometry was prepared by dropping an aliquot of the purified plutonium solution on Mylar film, drying it up, and covering it with Scotch tape. The spectrum measurement was started 40 days after bombardment. Among the impurities contained in the ^{237}Pu source, ^{236}Pu and ^{238}Pu, amounting to about 1% in the activities, were the most interfering for the decay measurement.

Four single peaks and two peak compounds which were not affected by the ^{236}Pu and ^{238}Pu activities were selected for constructing the decay curve of ^{237}Pu. The half-life value was deduced from each of the obtained decay curves by the least squares fit. The half-life value of 45.12±0.03 days was obtained as the weighted average of the six data.

Reference:

1) K. Hata, H. Baba, H. Umezawa, T. Suzuki, and T. Nozaki, Int. J. Appl. Rad. Isotopes 27 (1976) 713.

II. HIROSHIMA UNIVERSITY

Department of Physics, Faculty of Science

II-1

Precision Measurements of Gamma-Ray Intensities

Y. Yoshizawa, Y. Iwata, J. Takada, K. Kato* and M. Hoshi*

Relative gamma-ray intensities emitted from ^{124}Sb, ^{166m}Ho and ^{182}Ta were measured with Ge(Li) detectors. The detectors were calibrated within uncertainties of 0.5 % with standard sources and cascade gamma rays.[1] Intensities per decays were calculated by using relative intensities and internal conversion coefficients. The results of ^{124}Sb, ^{166m}Ho and ^{182}Ta are listed in Table I, II and III, respectively.

Reference :

1) Y. Yoshizawa, Y. Iwata, T. Kaku, T. Katoh, J. Ruan, T. Kojima and Y. Kawada, Nucl. Instr. and Meth. 174 (1980) 109

---

* Research Institute for Nuclear Medicine and Biology
Hiroshima University, Hiroshima 734

Table I. Relative intensities and intensities per decay of gamma rays for ^{124}Sb

Energy (keV)	Relative intensity (%)	Intensity per decay (%)	Energy (keV)	Relative intensity (%)	Intensity per decay (%)
370	0.051(9)	0.050(9)	1368	2.67(3)	2.61(3)
400	0.129(16)	0.127(15)	1376	0.501(20)	0.490(20)
444	0.205(10)	0.201(9)	1385	0.061(26)	0.060(25)
469	0.058(8)	0.057(8)	1437	1.225(24)	1.198(24)
526	0.117(12)	0.115(12)	1445	0.358(17)	0.351(17)
603	100.0(4)	97.83(5)	1489	0.679(19)	0.664(18)
632	0.114(6)	0.111(6)	1526	0.410(24)	0.401(24)
646	7.61(3)	7.44(4)	1580	0.433(12)	0.424(12)
663	0.016(5)	0.015(5)	1622	0.035(12)	0.034(12)
709	1.399(11)	1.368(12)	1691	48.58(16)	47.52(23)
714	2.338(12)	2.288(15)	1720	0.097(7)	0.095(7)
723	11.02(4)	10.78(6)	1919	0.052(4)	0.051(4)
736	0.133(9)	0.130(8)	2015	0.0093(26)	0.0091(25)
791	0.758(9)	0.741(9)	2039	0.0589(29)	0.0576(28)
817	0.079(6)	0.077(6)	2078	0.0163(25)	0.0159(24)
857	0.029(7)	0.029(7)	2091	5.589(22)	5.47(3)
900	0.016(9)	0.016(9)	2099	0.045(6)	0.044(6)
968	1.919(13)	1.877(14)	2108	0.0438(27)	0.0428(26)
976	0.088(8)	0.086(8)	2183	0.0398(19)	0.0389(19)
1045	1.864(17)	1.824(18)	2283	0.0041(13)	0.0040(13)
1086	0.038(9)	0.037(9)	2294	0.031(10)	0.030(10)
1263	0.046(15)	0.045(14)	2694	0.0027(19)	0.0026(19)
1301	0.041(15)	0.040(15)			
1325	1.584(22)	1.549(22)			
1355	1.042(27)	1.019(27)			

Table II. Relative intensities of gamma rays for ^{166m}Ho

Energy (keV)	Relative intensity (%)	Energy (keV)	Relative intensity (%)
94.653	0.270(30)	594.48	1.011(34)
135.238	0.169(18)	611.552	2.489(33)
140.618	0.056(18)	639.770	0.154(22)
160.064	0.164(16)	644.45	0.276(30)
161.748	0.166(16)	670.509	9.433(43)
184.407	124.4(12)	691.211	2.346(23)
190.711	0.379(20)	711.693	95.13(34)
214.763	0.755(50)	736.67	0.660(24)
215.875	4.44(7)	752.265	21.133(80)
231.282	0.359(15)	778.817	5.308(25)
259.716	1.843(29)	810.309	100.00(37)
280.456	51.43(25)	830.560	16.875(68)
300.744	6.425(33)	875.64	1.276(15)
339.78	0.289(22)	950.94	4.727(23)
365.739	4.285(30)	1010.25	0.129(8)
410.941	19.84(19)	1146.82	0.364(25)
451.524	5.175(31)	1241.44	1.353(39)
464.825	2.113(26)	1282.12	0.281(22)
529.813	16.745(85)	1400.72	0.873(33)
570.998	9.585(97)	1427.05	0.872(33)

Table III. Relative intensities and intensities per decay of gamma rays for ^{182}Ta

Energy (keV)	Relative intensity (%)	Intensity per decay (%)	Energy (keV)	Relative intensity (%)	Intensity per decay (%)
100.1	40.44(59)	14.30(21)	1157.2	1.66(24)	0.59(9)
110.4	0.25(6)	0.088(21)	1157.9	1.22(21)	0.43(7)
113.7	5.35(7)	1.89(2)	1180.7	0.212(36)	0.075(13)
116.4	1.26(3)	0.444(10)	1189.0	46.40(14)	16.40(7)
152.4	19.94(17)	7.05(6)	1221.4	76.80(59)	27.15(22)
156.4	7.60(6)	2.69(2)	1223.2	0.53(23)	0.19(8)
179.4	8.83(8)	3.12(3)	1231.0	32.72(10)	11.56(5)
198.3	4.22(5)	1.49(2)	1257.5	4.276(20)	1.511(8)
222.1	21.59(23)	7.63(8)	1273.8	1.87(1)	0.661(5)
229.3	10.49(11)	3.71(4)	1289.2	3.80(3)	1.342(12)
264.1	10.37(9)	3.67(3)	1342.7	0.723(7)	0.256(3)
351.1	0.034(19)	0.012(7)	1373.8	0.626(6)	0.2213(22)
829.5	0.038(15)	0.013(5)	1387.4	0.204(4)	0.0719(14)
891.9	0.162(45)	0.057(16)	1410.1	0.111(5)	0.0391(18)
928.0	1.764(38)	0.623(14)	1453.1	0.087(2)	0.0308(9)
959.7	0.978(45)	0.346(16)			
1001.7	5.85(10)	2.069(37)			
1044.4	0.719(74)	0.254(26)			
1113.4	1.296(33)	0.458(12)			
1121.3	100.00(30)	35.35(14)			

III. KYOTO UNIVERSITY

Research Reactor Institute

III-1

Measurement of Neutron Total Cross Section of ^{232}Th from Several meV to 20 eV

Katsuhei Kobayashi, Yoshiaki Fujita and Shigehiro Asano*

The neutron total cross section of ^{232}Th has been measured in the energy range from several meV to 20 eV by the linac TOF method. The transmission measurements were carried out with the samples given in Table 1 and with a ^{6}Li glass scintillation detector 12.7 cm in diameter and 1.27 cm thick located at the 22 m flight station.

The preliminary experimental result, which is shown in Fig.1, rather supports the ENDF/B-V data and recent measurements at RPI[1] and ORNL[2]. The ENDF/B-IV data is obviously lower than the present values. In very recent years, Ohsawa surveyed and evaluated the thorium cross sections[3], and the results will be incorporated in JENDL-2. The JENDL-2 data is rather close to the present values.

References :

1) R.C.Little, et al.: NP-1704 (1981).

2) D.K.Olsen and R.W.Ingle: ORNL/TM-7661 (1981).

3) T.Ohsawa and M.Ohta: J. Nucl. Sci. Technol., 18, 408 (1981).

* Kinki University
Kowakae, Higashi-osaka-shi, Osaka

Table 1 Transmission samples of thorium metal

Th - sample	Thickness cm	Thickness atom/barn
Open		
Sample-1	0.915	0.02648 ± 0.00004
Sample-2	2.128	0.06424 ± 0.00005
Sample-3	3.666	0.11009 ± 0.00006

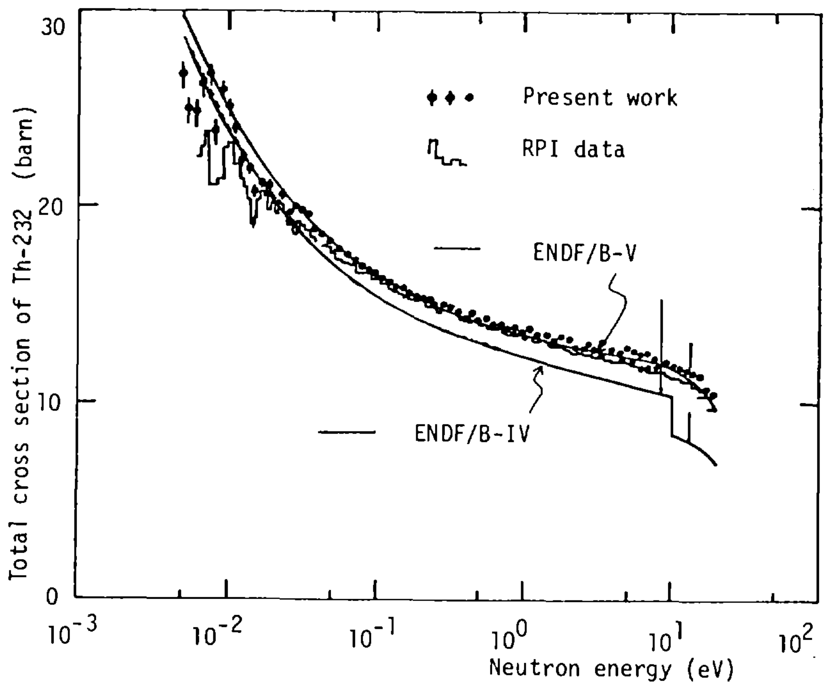

Figure 1 Total cross section of ^{232}Th

III-2

Assessment of Group Constants of ^{232}Th with Neutron Spectra scattered by Thorium Slab and measured in a Thoria Pile

Katsuhei Kobayashi, Takamasa Mori* and Itsuro Kimura

Neutron energy spectrum scattered by a thorium slab has been measured from several keV to several MeV by the linac time-of-flight method. The energy spectrum of neutrons in a spherical thoria pile was also measured previously by the authors. The detail is given in the literature[1]. The measured results have been compared with the theoretical ones by the transport calculation code DTF-IV. The group constants of ^{232}Th used for the calculation were produced from ENDF/B-IV and JENDL-2 with the processed code SUPERTOG.

The measured and calculated results from the thorium slab and the thoria pile are shown in Fig.1 and Fig.2, respectively. General agreement between measurements and calculations was seen for both spectra. The predicted spectra are rather lower than those measured in the MeV energy region. Especially, the spectra calculated with constants from JENDL-2 data give much less neutron flux by about 10 % than those from ENDF/B-IV data above about 1 MeV.

By substituting the thorium constants from JENDL-2 for those from ENDF/B-IV, it has been found that one of the main sources of the less neutron fluxes with JENDL-2 data may be due to the smaller inelastic scattering cross sections of ^{232}Th in the JENDL-2.

Reference :

1) H.Nishihara, et al.: J. Nucl. Sci. Technol., 14, 426 (1977).

* Department of Nuclear Engineering, Kyoto University
Yoshida-honmachi, Sakyo-ku, Kyoto-shi

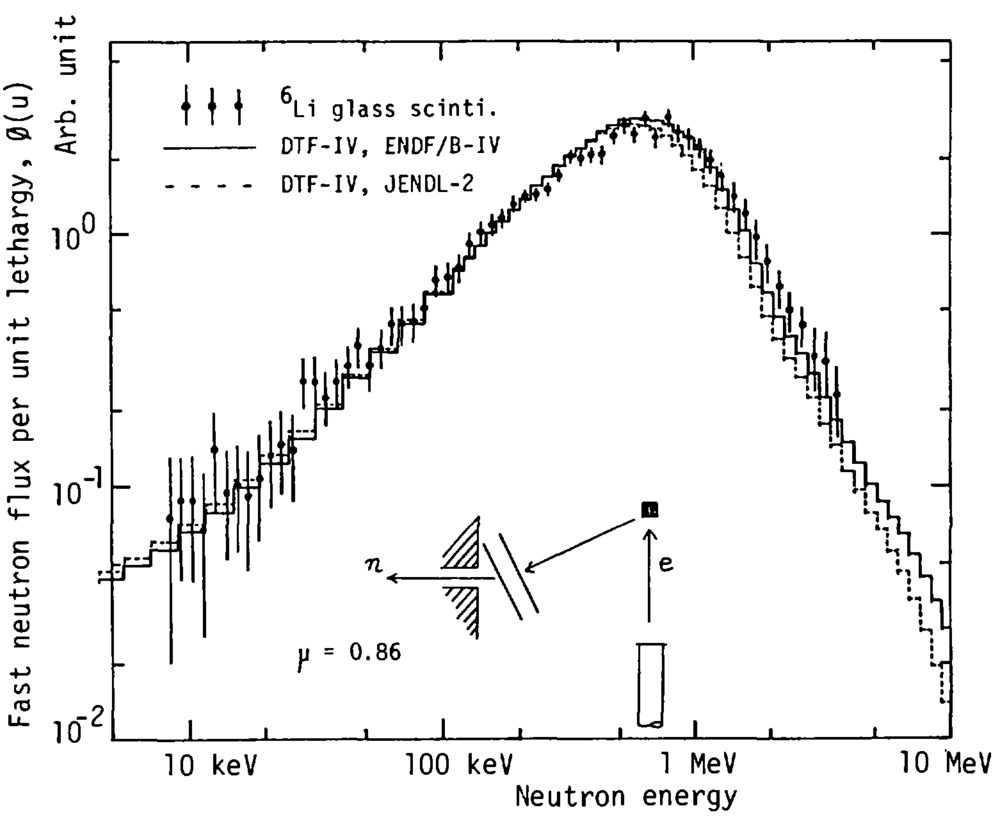

Fig. 1 Neutron energy spectra scattered by a thorium slab

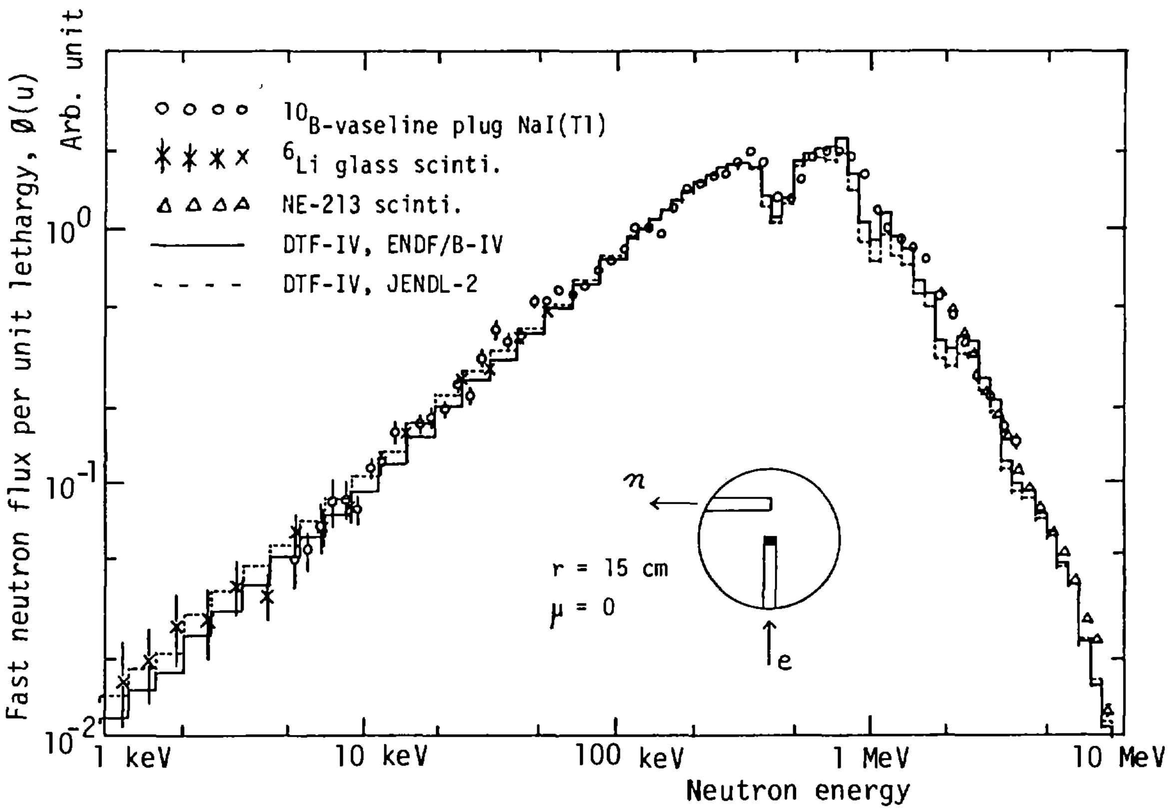

Fig. 2 Neutron energy spectra in a thoria pile

III-3

Covariances in the Measurement of Californium-252 Spectrum Averaged Cross Sections

Katsuhei Kobayashi, Itsuro Kimura and Wolf Mannhart *

A paper on this subject will be submitted to the J. Nucl. Sci. Technol.

The ^{252}Cf fission spectrum averaged cross sections of twelve reactions have been measured relative to that of the ^{27}Al(n,α)^{24}Na reaction. The present work is a continuation of our recent measurement[1]. The uncertainties of the measurement are analyzed with regard to the covariances of experimental data. It is demonstrated how to generate and combine the experimental uncertainties in the form of a variance-covariance matrix. The results of the averaged cross sections and of the uncertainty analysis taking account of correlations between the experimental data are given in Table 1. A non-diagonal weighted least square fit has been applied to normalize the measured ratio. The standard deviation obtained by the present analysis has been reduced to almost half compared with the processed previously using variances of the average cross section presented here are compared with the calculated ones based on the energy dependent cross sections.

---

* Physikalisch-Technische Bundesanstalt
33 Braunschweig, Federal Republic of GERMANY

Reference :

1) K. Kobayashi and I. Kimura : Proc. of the Third ASTM-EURATOM Symp. on Reactor Dosimetry, Ispra, EUR-6813, Vol.II, p.1004 (1980).

Table 1 Present results of the Cf-252 spectrum averaged cross sections and the correlations between them

Reaction	<σ> (mb)	Std.dev.(%)	Correlation matrix (x 100)												
$^{24}Mg(n,p)^{24}Na$	1.940	4.79	100												
$^{27}Al(n,p)^{27}Mg$	4.891	3.67	40	100											
$^{27}Al(n,\alpha)^{24}Na$	1.006	2.17	44	58	100										
$^{32}S(n,p)^{32}P$	72.52	4.08	41	45	52	100									
$^{51}V(n,p)^{51}Ti$	0.7126	8.25	14	26	25	16	100								
$^{54}Fe(n,p)^{54}Mn$	87.63	4.97	46	41	42	40	16	100							
$^{56}Fe(n,p)^{56}Mn$	1.440	4.86	47	42	43	41	16	53	100						
$^{58}Ni(n,p)^{58}Co$	118.5	3.45	39	55	62	50	24	40	41	100					
$^{59}Co(n,\alpha)^{56}Mn$	0.2176	6.44	19	31	33	23	17	20	21	28	100				
$^{64}Zn(n,p)^{64}Cu$	41.84	4.18	29	46	51	36	23	30	30	42	29	100			
$^{113}In(n,n')^{113m}In$	169.7	4.77	48	46	44	39	20	49	50	45	22	30	100		
$^{115}In(n,n')^{115m}In$	201.0	4.08	56	54	52	46	24	60	61	53	26	36	66	100	
$^{197}Au(n,2n)^{196}Au$	5.267	4.30	28	49	50	31	29	32	33	46	32	45	39	47	100

* Normalized with <σ>(Al-27(n,α)) = 1.006 mb ± 2.2 %

III-4

Measurement and Analysis of Energy Spectra of Neutrons in Structural Materials for Reactors

Itsuro Kimura, Shu A. Hayashi, Katsuhei Kobayashi,
Shuji Yamamoto, Hiroshi Nishihara *, Takamasa Mori *,
Masayuki Nakagawa **

In order to assess neutron cross sections or group constants of main structural materials for reactors, measurement and analysis of neutron spectra in sample piles have been continuously carried out actively.

After the invited paper at the last Knoxville Conference [1), molybdenum, niobium, nickel and chromium have been studied. The fisrt two elements are thought to be materials for high temperature reactors and fusion reactors. The last two and iron are the main constituents of stainless steel. The studies for iron and stainless steel itself were performed previously, but the results are being reanalyzed with JENDL-2 data. In analysis of all other materials, we are using JENDL-2 and ENDF/B-IV data unless it is available.

The result for molybdenum will be submitted to J. Nuclear Science and Technology soon.

Reference :

1) I. Kimura, Proc. Conf. Nuclear Cross Sections for Technology NBS Sp. Publ. 594, p. 265 (1980).

---

* Department of Nuclear Engineering, Kyoto University

** Japan Atomic Energy Research Institute

IV. KYUSHU UNIVERSITY

A. Department of Nuclear Engineering
Faculty of Engineering

IV-A-1 Analysis of Total 14 MeV (n,α) Cross Sections with Pre-Equilibrium Model and Effective Q-values

I. Kumabe

Recently author[1)] has analyzed the measured cross sections of 14 MeV (n,p) reaction for nuclei with mass number larger than 90 in terms of the pre-equilibrium exciton model[2)] and an effective Q-value, that is derived from a semi-empirical mass formula whose parameters are smooth functions of mass number and are free from fluctuations near closed shells. The deviations from 1.0 of the ratios of experimental to theoretical cross sections calculated using the effective Q-values are markedly reduced as compared with the use of the true Q-values. We have demonstrated[1)] that the use of the effective Q-value is reasonable for the pre-equilibrium process using the uniform spacing shell model modified by the shell effect.

Similar analysis for the 14 MeV (n,α) reaction is very interesting.

The ratios of the experimental to theoretical cross sections calculated using the pre-equilibrium model[3)] and the true Q-values are plotted in the upper part of Fig. 1. In this figure gross mass-number dependence of the ratios is seen.

Levkovskii[4] has presented the most reliable averaged values of the 14 MeV (n,α) cross sections. However the data for nuclei with mass number A=140~167 are absent in his evaluated cross sections. Therefore we have evaluated the most reliable averaged values for nuclei with A=140~167. These experimental cross sections have been used in the present analysis.

We define the quantity $Q'=Q-\delta_r+\delta_t$ as an effective Q-value for the (n,α) reaction. Here Q is the true Q value, and δ_r and δ_t are the depressions of the ground state energies of the residual and target nuclei, respectively, producing by pairing and shell correlations. If pairing and shell energies are taken from Cameron and Elkin[5], the effective Q-values do not vary smoothly with the mass number A. Therefore the effective Q-value is calculated as follows. Since the Q-value for the (n,α) reaction on a given element decreases linearly with the mass number, it can be approximated by a straight line. The approximate Q-value, therefore, is expressed as

$$Q' = B(A - A_0) + 6.0 \text{ MeV}, \qquad (1)$$

where B is the slope of the straight line and A_0 is the mass number at which the straight line intersects with Q=6 MeV.

The values of A_0 and B for each element can be determined from least squares analysis of the corresponding Q value. The values of A_0 and B were plotted as a function of atomic number Z. The Z-dependence of A_0 and B seems to have considerable structures near closed shells. In order to approximate shell-independent values of A_0 and B, we have fitted the points by least squares procedure using quadratic functions of Z. The smoothed values of A_0 and B are

$$A_0 = 0.00995Z^2 + 1.865Z - 3.08, \quad (2)$$

$$B = -0.000203Z^2 + 0.0301Z - 1.47. \quad (3)$$

From equations (1), (2) and (3) the effective Q-value can be easily calculated as functions of A and Z.

The ratios of the experimental to theoretical cross sections calculated using the effective Q values are plotted in the middle part of Fig. 1. The A-dependence of the points seems to be just opposite to that using the true Q-values. The use of the averaged cross section $(\sigma^t_{cal}+\sigma^e_{cal})/2$ is expected to achieve good results, where σ^t_{cal} and σ^e_{cal} are the cross sections calculated using the true and effective Q-values, respectively.

The ratios of the experimental to the averaged cross sections are plotted in the lower part of Fig. 1. The deviations of the points from 1.0 are markely reduced. Since the errors for the experimental cross sections are considered to be 10~30 %, the caluclated cross sections are thought to be in good agreement with the experimental ones.

The uniform spacing shell model is used in the pre-equilibrium model. It has been well known in the usually used shell model with spin-orbit coupling that the large energy jumps of orbit spacings occur at the magic numbers. Taking this shell effect into account, we modify the uniform spacing shell model. This modified shell model is same as that used for the (n,p) reaction[1].

Under the assumption of the one-step direct (n,α) reactions, an incident neutron picks up one neutron and two protons in occupied orbit. On the basis of the theoretical consideration using the modified shell model, we have demonstrated that the use of the averaged cross section $(\sigma^t_{cal}+\sigma^e_{cal})/2$ is reasonable for the pre-equilibrium (n,α) process.

We have calculated the theoretical cross sections using the averaged Q value (Q+Q')/2 of the ture Q-value Q and the effective Q-value Q', and have obtained similar results to those, for the averaged cross section, shown in the lower part of Fig. 1. In the present calculation we have used the constant value of 0.18 as a coefficient φ defined in ref. (3).

References

1) I. Kumabe, J. Nucl. Sci. Technol. 18 (1981) No. 8 to be published, NEANDC(J)-61/U p. 92 (1979).

2) G.M. Braga-Marcazzan et al., Phys. Rev. C6 (1972) 1398.

3) L. Milazzo-Colli et al. Nucl. Phys. A210 (1973) 297.

4) V.N. Levkovskii, Sov. J. Nucl. Phys. 18 (1974) 361.

5) A.G.W. Cameron and R.M. Elkin, Can. J. Phys. 43 (1965) 1288.

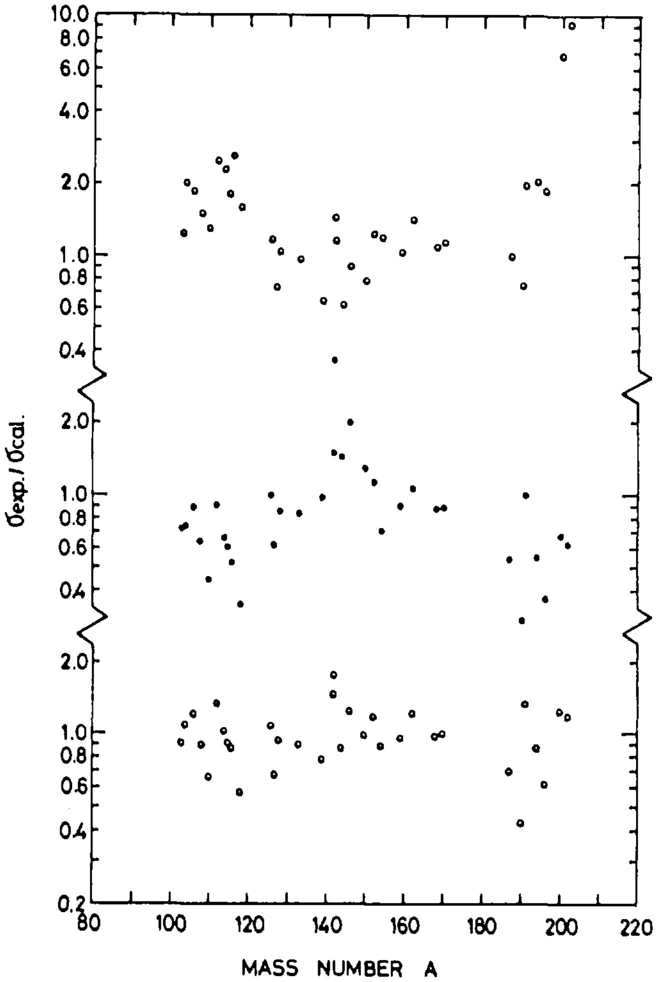

Fig. 1 Ratios of experimental to theoretical cross sections calculated using true Q-values and effective Q-values plotted in upper and middle parts, respectively. Ratios of experimental to averaged cross sections $(\sigma_{cal}^{t}+\sigma_{cal}^{e})/2$ plotted in lower parts.

IV-A-2 Analysis of energy spectra of particles emitted from the reaction of 14 MeV neutrons on nuclei with A = 40 ~ 70

M. Hyakutake, M. Haruta and I. Kumabe

In the mass-number region of 40~70, multi-particles emissions including charged particles become important in the calculation of cross sections at incident neutron energy above about 10 MeV. For the calculation of these cross sections it is necessary to take into account the competition between the γ-ray and the particle emission, and also the pre-equilibrium process. Recently, Kumabe has reported the analysis of the 14 MeV (n,p) and (n,α) cross sections for nuclei with mass number larger than 90 using the pre-equilibrium model and an effective Q-value, and showed the good agreement between experimental and calculated cross sections[1].

In the present report we have analysed the energy spectra of neutron, proton and alpha particle emitted from the reaction of 14 MeV neutrons using the following models and parameters, and compared with experimental data of Grimes et al[2].

a. the inclusion of neutron, proton, alpha particle and γ-ray for decay channels

b. the evaporation model and the level density of Gilbert and Cameron for the equilibrium process

c. the exciton model and the effective Q-value[1] for the pre-equilibrium process

The energy spectra of the neutron, proton and alpha particle for nuclei from Ti to Cu were calculated under these assumptions. For proton emission in the pre-equilibrium process the effective Q-value was used. On the other hand for alpha particle emission in the pre-equilibrium process the averaged effective Q-value $Q'=(Q_e+Q_t)/2$ of the effective Q-value Q_e and the true Q-value Q_t. In Fig. 1 is shown typical proton and

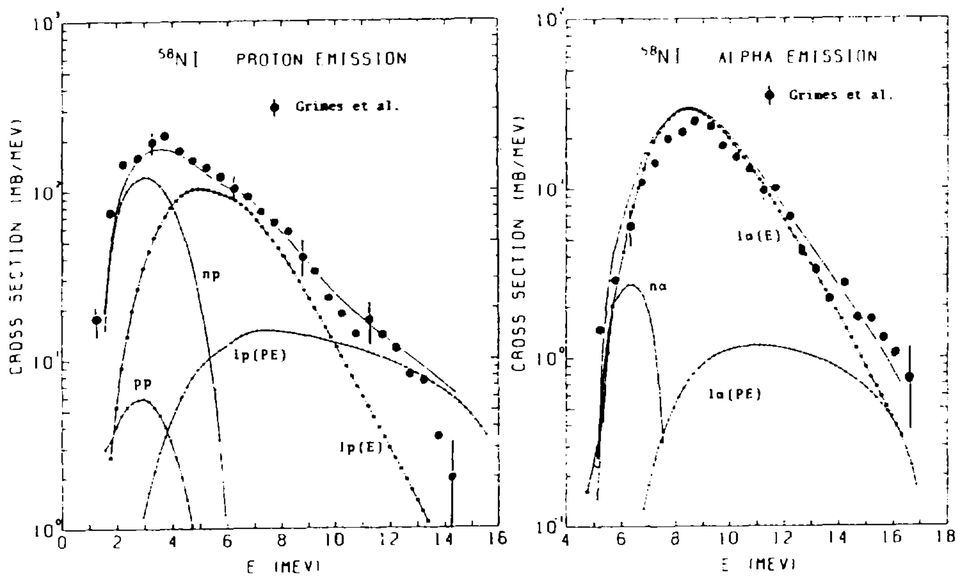

Fig. 1 Calculated and experimental proton and alpha particle emission spectra from 14 MeV neutrons on Ni^{58}. E : equilibrium process, PE : pre-equilibrium process, 1p(α) : 1-st proton (alpha) emission, np(α) : protons (alpha particles) after 1-st neutron emission, pp : protons after 1-st proton emission.

alpha emission spectra calculated for Ni^{58}. The agreement between the measured and calculated values is good. The agreement between the measured and calculated values was generally good for other targets.

References :

1) I. Kumabe, J. Nucl. Sci. Technol. 18 (1981) No. 8 to be published, NEANDC(J)-61/U p. 92 (1979) and preceeding report

2) S.M. Grimes et al., Phys. Rev. C19 (1979) 2127 and references contained therein

IV-A-3

Neutron Nuclear Data Evaluation for Thorium-232

T. Ohsawa and M. Ohta

A paper on this subject was published in Journal of Nuclear Science and Technology, Vol.18, No.6, pp.408-426 (1981), with an abstract as follows:

An evaluation was made on the neutron cross sections, resonance parameters and average neutron yield in fission for ^{232}Th in the energy range from thermal energy to 20 MeV. The fission and capture cross sections were evaluated on the basis of the experimental data by converting the relative ratio data into cross section values by making use of recent evaluations for reference cross sections. The total cross section was determined from experimental data in the region from 24 keV to 15 MeV and then extrapolated to lower and higher energies by using the optical model whose parameters had been adjusted as so to reproduce the measured data. The elastic and inelastic scattering, $(n,2n)$ and $(n,3n)$ reaction cross sections were calculated by means of the statistical model combined with the optical model. A set of resonance parameters were recommended in the energy range below 3.5 KeV and average resonance parameters were deduced in the unresolved resonance region. A value of 7.40b was chosen for the capture cross section at 0.025eV, and the picket-fence negative-energy levels were introduced so as to reproduce the non-$1/v$ behavior of the capture cross section in the epithermal region.

The results were incorporated in the Japanese Evaluated Nuclear Data Library, Version 2 (JENDL-2). Comparison was made between the present and other evaluations such as ENDF/B-V and possible reasons for the discrepancy were discussed.

IV-A-4

Neutron Nuclear Data Evaluation of Rare Isotopes of Thorium: ^{228}Th, ^{230}Th, ^{233}Th and ^{234}Th

T. Ohsawa snd M. Ohta

A paper on this subject was published in Memoirs of the Faculty of Engineering, Kyushu University, Vol.40, No.3, pp.149-166 (1980), with an abstract as follows:

La necessité d'une connaissance des section efficaces neutroniques sur isotopes rares de thorium apparait à l'examen des demandes de données nucléaires pour les réacteurs utilisant thorium.

Afin d'obtenir des renseignements sur les données de l'interaction de neutrons avec les isotopes rares de thorium pour enregistrer dans la bibliothèque japonaise de données nucléaires JENDL-2, un ensemble de calculs de données neutroniques a été entrepris dans la gamme d'énergie allant de l'énergie thermique à 20 MeV. Il se compose des calculs de sections efficaces totale,de diffusions élastique et inélastique,de capture radiative, de fission et de réactions $(n,2n)$, $(n,3n)$, et nombre moyen de neutrons prompts pour les noyaux Th-228, Th-230, Th233 et Th-234.

L'analyse théorique de capture radiative et d'excitation des niveaux inélastique a été effectuée á l'aide du modèle ststistique de Moldauer couplé avec modèle optique. La section efficace de fission a été obtenue par une méthode de calcul en utilisant des données de probabilité de fission fournies par les mesures expérimentaux. Les sections efficaces de réactions $(n,2n)$ et $(n,3n)$ sont calculées par le formalisme de Segev et Caner,et le nombre moyen $\overline{\nu}_p$ de neutrons prompts par la méthode semi-empirique de Howerton.

Les résultats d'évaluation sont présentés avec les paramètres nucléaires utilisés dans les calculs.

IV-A-5

Double-Humped Barrier Model Analysis of Fission Cross Secrions for Actinide Nuclei

T. Ohsawa, M. Mine, M. Ohta and K. Kudo

A paper on this subject was published in Memoirs of the Faculty of Engineering, Kyushu University, Vol.41, No.2, pp.143-164 (1981), with an abstract as follows:

A double-humped fission barrier model was applied to the analysis of neutron-induced fission cross section of 28 actinide nuclides and information on the barrier heights was deduced. For nuclei with $Z \geqq 91$, good fits to measurements were obtained by assuming that the first barrier is mass-symmetric and axially asymmetric while the second barrier is mass-asymmetric and axially symmetric. For thorium isotopes, for which both the first and second barriers are mass-asymmetric and axially symmetric, introduction of an additional barrier C which has mass-symmetry but not axial symmetry was found to give better agreement between theory and experiments. Systematic trends were observed in the barrier heights of the nuclei when regarded as a function of neutron number.

B. Interdisciplinary Graduate School of Engineering Sciences

IV-B-1

Self-shielding on Transmission Measurements in Unresolved Resonance Region

I. Tsubone , Y. Kanda , Y. Nakajima*

In the measurements of total cross section in the unresolved resonance region, the influence of self-shielding and Doppler effect on transmission measurements have to be taken into account. We have simulated these effects in the experiments of total cross section for ^{238}U using the computer code TIMS-1[1)] which is programed originally by Takano et al., and is modified slightly by us.

The resonance parameters and level spacings which obey the Poter-Thomas and Wigner distribution respectively, are generated up to a few handred keV by using average resonance parameters and Monte-Carlo method.

In the code, the Doppler broadened total cross section $\sigma_{tD}(E)$ are calculated. Then we have calculated effective average total cross section (EATCS) as follow

$$\sigma(n) = -\frac{1}{n} \ln\left[\int_{\Delta E} e^{-n\,\sigma_{tD}(E)}\, dE \Big/ \int_{\Delta E} dE \right]$$

where n is sample thickness.

The limitation selecting the ladders of resonance parameters was set to 0.01, after the variations of EATCS with different random starters were checked up.

Energy dependency of self-shielding in EATCS have been calculated. It appears that a little influence still remains until 200 keV as shown in fig-1.

* Japan Atomic Energy Research Institute

The dependency of EATCS on the temparature have been calculated, and their results are shown in fig-2. As they varies gradually above 200 K and the influence of Doppler effect at this part are negligibly small, we conclude that room temparature is sufficient for measurements.

The calculated EATCS for sevral average resonance parameter sets have been compared.

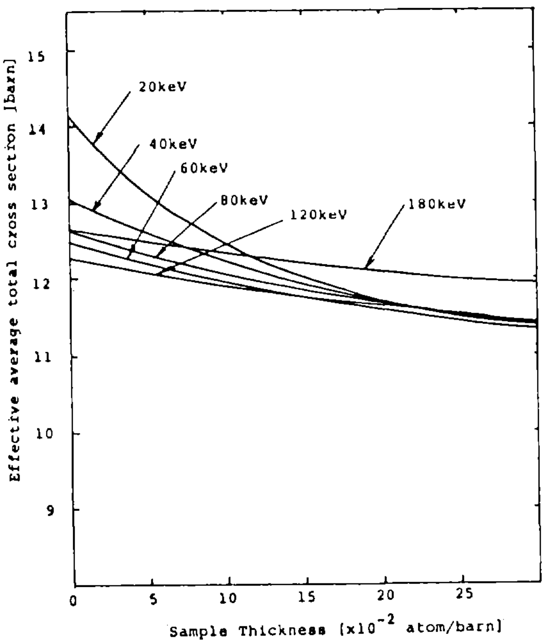

Fig-1 : Energy dependency of self-shielding of EATCS.

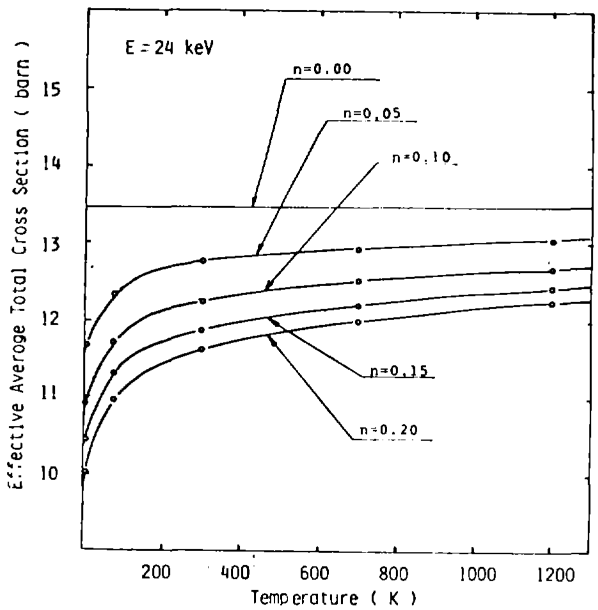

Fig-2: Temparature dependency of EATCS, where n is sample thickness (atom/barn).

Reference :

1) Takano et,al., JEARI-1267 (1980)

IV-B-2

Measurements of Total Cross Section of ^{238}U in the keV Region

I. Tsubone , Y. Kanda , Y. Nakajima*, Y. Furuta*

Measurements of total cross section of ^{238}U in the keV region are in progress with transmission method, using the time of flight spectrometer of the Japan Atomic Energy Research Institute 120 MeV electron linac with 100-m flight path. An Fe-filtered neutron beam technique and a Li-glass scintillator which have high counting efficiency in keV region have been used.

About 20 bands of filtered neutrons in the energy range from 20 keV to 1 MeV are available for measuring the neutron transmission. An example of the time spectra of the neutron beam are shown in fig-1, where the upper curve is for the sample-out run and the lower is for the sample-in run.

The neutron transmission have been measured with four samples whose thickness are 0.00628, 0.02486, 0.04951 and 0.08066 atoms/barn, to observe the resonance self-shielding at lower range in the keV region.

Preliminary results have been obtained, and detail analysis are now carrying out with a computer FACOM M-200 in Kyushu University.

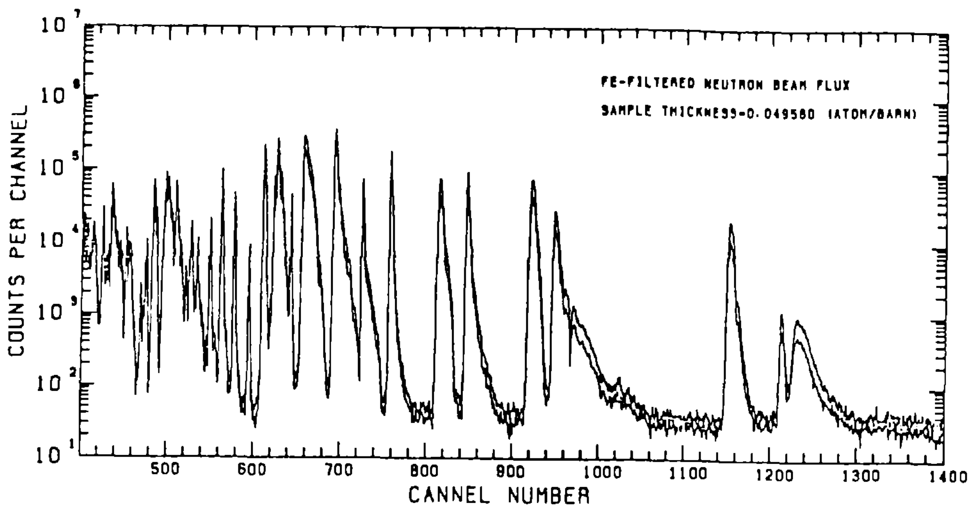

Fig - 1

* Japan Atomic Energy Research Institute

IV-B-3

The statistical method of simultaneous evaluation for nuclear data

Y.Uenohara and Y.Kanda

Experimental cross sections can be categolized into two cases. The ones are measured as the absolute values or as the ratio to the well evaluated standard cross sections;they are called the absolute data. The others are measured as the values of the cross section ratio relative to other cross section ;they are called the relative data. Usually,the evaluation of the cross sections are performed by using both the absolute data and the absolute value to which are normalized from the relative data. It is prefered generally that the measured data are used their own in the evaluation. On the other hand,recently the covariances to the evaluated nuclear data desired. Therefore,it is necessary to obtain evaluated nuclear data and the covariances for them by using absolute data and relative data simultaneously.

We have tried to evaluate a few kind of the cross sections simultaneously by combining "roof function"[1)] with the linear least square method in which the logarithms of the experimental data are used to linearize the cross section ratios. This method includes the requirements described in the last paragraph.

In this report,we present preliminary results for $\sigma_f(^{235}U)$,$\sigma_f(^{238}U)$ and their ratios only to show the utilization of the method. The results given in Figs.1,2,and 3 have been obtained by using the experimental data selected arbitrarily. The bands along the evaluated curves which correspond to one standard deviation are calculated from the covariances resulted from the least square method.

Reference

1) F.Schmitroth and R.E.Schenter; Nucl.Sci.Eng: 74 168 (1980)

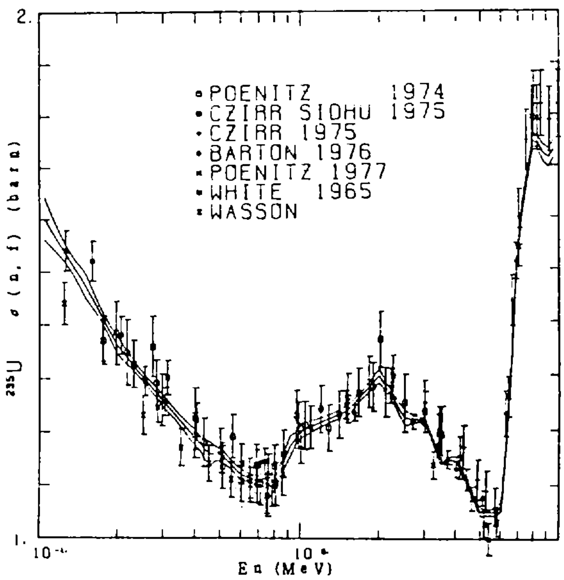

Fig.(1)

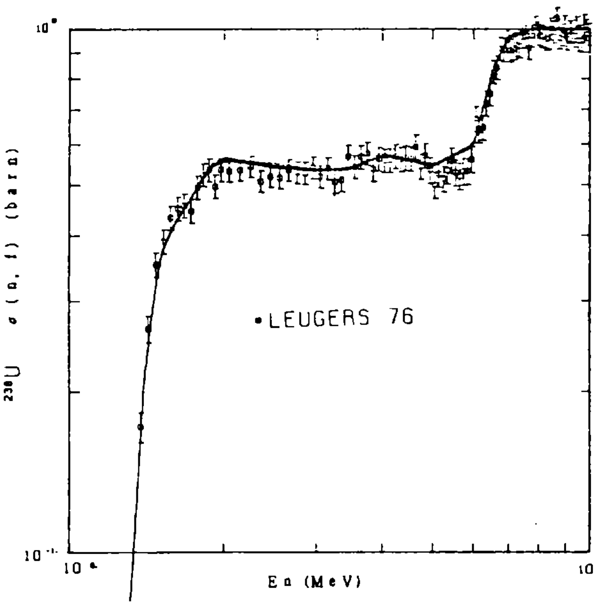

Fig.(2)

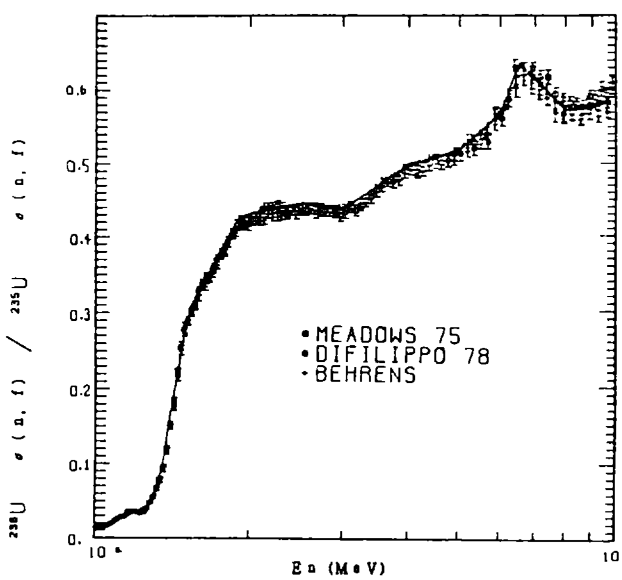

Fig.(3)

V. NAGOYA UNIVERSITY

Department of Nuclear Engineering

V-1 Decay Properties of ^{145}Ce and ^{146}Ce

H. Yamamoto, Y. Ikeda, K. Kawade, T. Katoh and T. Nagahara*

A paper on this subject has been published in J. Inorg. Nucl. Chemistry vol.42 p. 1539(1980) with an abstract as follows :

Gamma-ray singles, γ-γ coincidence, β-ray singles, β-γ coincidence and half-life measurements have been performed to study decay properties of ^{145}Ce and ^{146}Ce by using a rapid electrophoresis. Thirty-two γ-rays from ^{145}Ce, including 14 new ones, and 26 γ-rays from ^{146}Ce, including 6 new ones, were observed, and 25 γ-rays and 21 ones were assigned to the decay schemes for ^{145}Ce including 3 new levels and for ^{146}Ce, respectively. The half-lives of ^{145}Ce and of ^{146}Ce are 3.01±0.06 and 13.52±0.13 min, and observed Q_β values for ^{145}Ce and for ^{146}Ce are 2.6±0.1 MeV and 952±50 keV, respectively.

---

* Institute for Atomic Energy, Rikkyo University

V-2 Decay Studies of ^{143}La and ^{147}Pr

H. Yamamoto, Y. Ikeda, K. Kawade, T. Katoh and T. Nagahara*

A paper on this subject has been published in J. Inorg. Nucl. Chemistry vol.43 p.855(1981) with an abstract as follows :

The decay properties of ^{143}La and ^{147}Pr were investigated with Ge(Li), NaI(Tl) and plastic detectors in singles and coincidence modes with the help of a rapid paper electrohoresis. Twenty-three new γ-rays for ^{143}La and 9 new transitions for ^{147}Pr were observed and fairly precise decay schemes for ^{143}La including 5 new levels and for ^{147}Pr including 4 new levels were proposed. The half-lives of ^{143}La and ^{147}Pr are 14.14±0.16 and 13.3±0.4 min and observed Q_{β} values for ^{143}La and ^{147}Pr are 3.28±0.10 and 2.77±0.10 MeV, respectively.

---

* Institute for Atomic Energy, Rikkyo University

VI. Osaka University

Faculty of Engineering

VI-1

Measurements of Double Differential Total Neutron Emission Cross Sections with 14 MeV Incident Neutrons for C, Li, Al and Pb

A. Takahashi, J. Yamamoto and K. Sumita

A program of double differential total neutron emission cross section (DDX) measurements for fusion reactor materials is under way at the intense 14 MeV neutron source facility (OKTAVIAN) of Osaka University.

Secondary neutron spectra for several scattering angles from a ring sample were measured by means of the TOF technique (see Fig.1). D-T neutron bursts of 1.5 ns pulse width in FWHM were used. Angular distribution of D-T neutron yield from the target assembly was defined by the Al(n,α) rate measurement. Correlation between mean source neutron energy and angle was obtained by the TOF data of elastic scattering for a lead ring (see Fig.2). These source neutron conditions were used for corrections in deriving DDX data to be compared with the data reproduced from ENDF/B-IV.

Scattering angle was varied with the distance between the target and a ring sample. TOF measurement was possible for laboratory scattering angle of 15 to 160 degree. Back ground run was done by just taking out the ring sample. Data normalization among several TOF runs was performed by counting the burst D-T neutrons with a 2"ϕx2" NE213 detector positioned at 90 degree and 3 meters from the target. The main neutron detector of 5"ϕx2" NE213 was located at 8.65 meters from the target. Diameters of ring samples were about 20 cm at most. An example of raw TOF data is shown in Fig.3.

Energy-dependent efficiency of the 5"x2"NE213 detector was measured by the Cf-252 TOF experiment for 0.5 to 8 MeV and in addition by the polyethylene ring-TOF experiment (based on elastic scattering by hydrogen) for 6 to 14 MeV. DDX value in barns/steradian/MeV will be derived with the polyethylene-ring-TOF experiment, by using hydrogen cross sections as standard. However the preliminary results shown here were normalized to the differential elastic scattering cross sections (barn/steradian) of ENDF/B-IV table at the most forward scattering angle measured for each sample. DDX data for 7 to 6 angle-points were preliminarily obtained for natural-lithium, carbon, alminum and natural-lead which are important for fusion application.

Carbon; Figure 4 shows an example of results, in comparison with the reproduced[1)] DDX from ENDF/B-IV[2)]. From the comparisons for all angles, we confirmed that all inelastic secondary neutrons were resulting from level-excitations and followed by level-scattering kinematicses, and that there appeared, therefore, disagreements with ENDF/B-IV data for the higher levels than the first. Resolved four differential level-cross-sections, including elastic, are listed in Table-1 with reference ENDF/B-IV and BNL-400 data. It should be noted here that the present experment gave 10 to 50 % larger values for the first level and 30 to 80 % smaller values for the higher two levels than the references.

Natural-lithium: An example is shown in Fig.5. Comparisons with the reproduced DDX data from ENDF/B-IV[3)] led us to the same conclusion with that for carbon. The second level inelastic scattering by Li-7 (Q=-4.63 MeV) was clearly resolved in the measurement. All inelastic secondary neutrons showed strong anisotropies in the Laboratory system. It shows the necessity of level scattering concept which is not the case for ENDF/B-IV, for all possible inelastic excitation levels.

Alminum : Fairly good agreements were attained between experiments and ENDF/B-IV data, particularly for the higher energy range where ENDF/B-IV[4] has differential level cross sections evaluated properly, as shown in Fig.6. However, more analyses in detail should be done for the lower energy range (than 9 MeV in Fig.6, for example) where the "pseudo-levels" were adopted in the ENDF/B-IV data.

Lead : Measured DDX showed remarkable disagreements with the reproduced DDX data from ENDF/B-IV[5], as shown in Fig.7, in the whole energy range and angles. This may suggest the predominant contribution of direct and pre-equilibrium processes for inelastic and (n,2n) reactions. Experiments showed remarkable forward-scattering of non-elastic neutrons in the wide energy range (14 to 1 MeV).

These results will be presented at the 1981 Fall Meeting of JAES which will be held at Kyushu University.

References :

1) Yamamoto, J., et al. : "Neutron transport calculations by the NITRAN system with double differential cross sections", submitted to J. Nucl. Sci. Technol.

2) MAT 1274, evaluation by Perey, F. G. and Fu, C. Y. (ORNL)

3) MAT 1274, evaluation by Labouve, R. J., et al. (LASL)

4) MAT 1193, evaluation by Young, P. G., et al. (LASL)

5) MAT 1288, evaluation by Fu. C. Y., Perey, F. G. (ORNL)

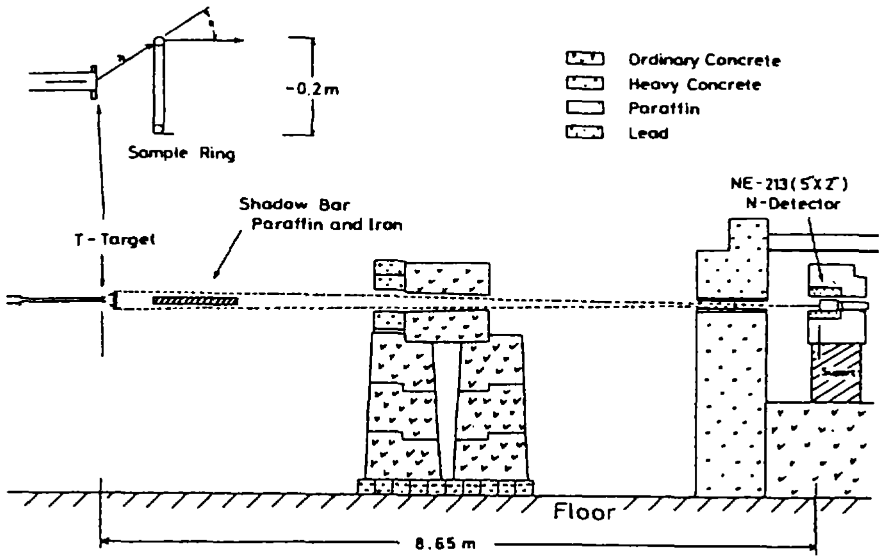

Fig.1 : Experimental arrangement for ring sample & TOF

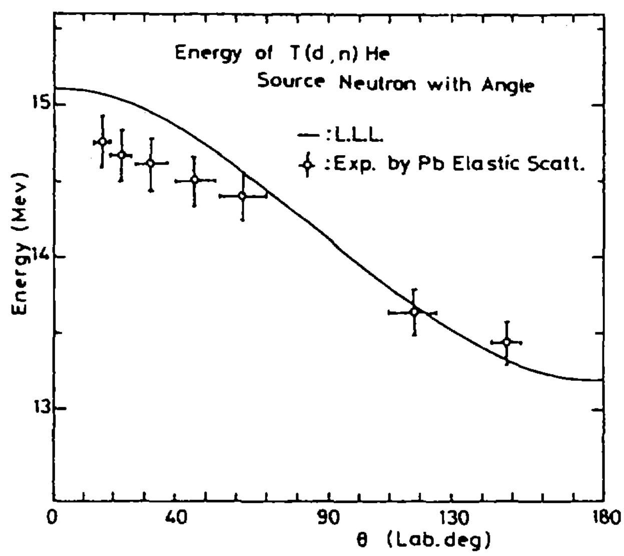

Fig.2 : Angular dependence of source neutrons

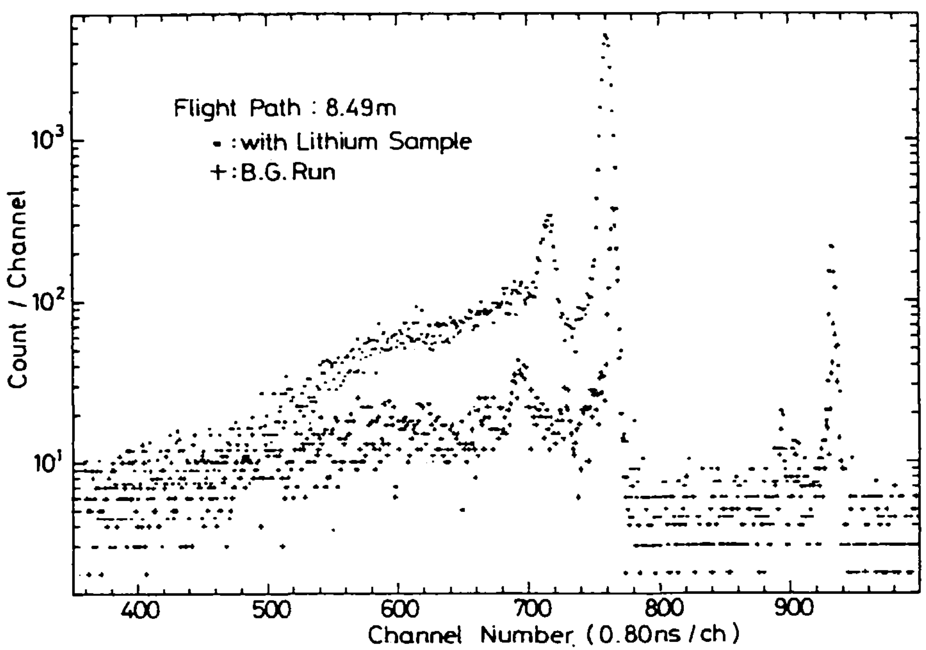

Fig. 3 : Example of raw TOF data, for Li sample & BG run

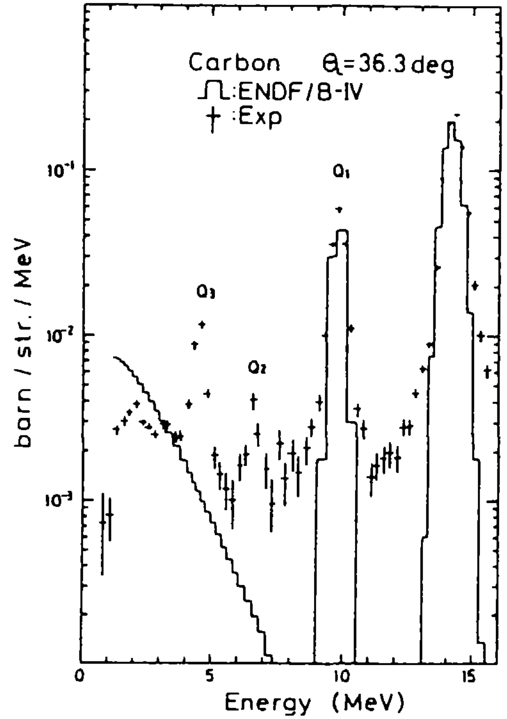

Fig.4 : DDX for carbon at 36.3 deg.(LAB)

Tabel 1 Carbon Level Cross Sections (Lab. system)
(barn /str.)

θ_L	Elastic scattering		Inelastic scattering (Discrete level)					
			-4.43 MeV		-7.66 MeV		-9.63 MeV	
(deg)	Exp.	B/IV	Exp.	B/IV	Exp.	ENDL + BNL-400	Exp.	ENDL + BNL-400
18.4	4.30E-1 ± 4E-3	4.31E-1	4.67E-2 ± 1.2E-3	4.34E-2	4.10E-3 ± 5.9E-4	7.80E-3	8.50E-3 ± 5.1E-4	1.38E-2
25.5	3.55E-1 ± 2E-3	3.44E-1	4.81E-2 ± 9E-4	3.90E-2	4.20E-3 ± 4.0E-4	5.00E-3	9.02E-3 ± 3.8E-4	1.35E-2
36.3	1.91E-1 ± 1E-3	1.56E-1	3.80E-2 ± 6E-4	3.10E-2	3.16E-3 ± 3.0E-4	1.63E-3	7.65E-3 ± 2.1E-4	1.27E-2
50.7	5.90E-2 ± 6E-3	3.37E-2	3.00E-2 ± 4E-4	2.00E-2	7.60E-4 ± 8.0E-5	8.56E-4	5.95E-3 ± 1.2E-4	1.10E-2
114.0	3.39E-2 ± 4E-3	3.09E-2	1.73E-2 ± 3E-4	1.28E-2	5.07E-4 ± 3.2E-5	1.33E-3	3.50E-3 ± 7E-5	6.02E-3
143.7	1.63E-2 ± 5E-3	8.98E-3	1.35E-2 ± 4E-4	2.00E-2	3.16E-4 ± 1.8E-5	1.46E-3	1.85E-3 ± 9E-5	3.11E-3

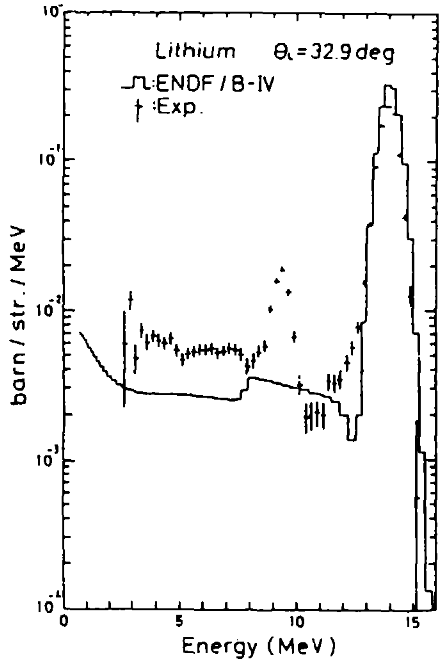

Fig.5 : DDX for nat. Li at 32.9 deg.(LAB)

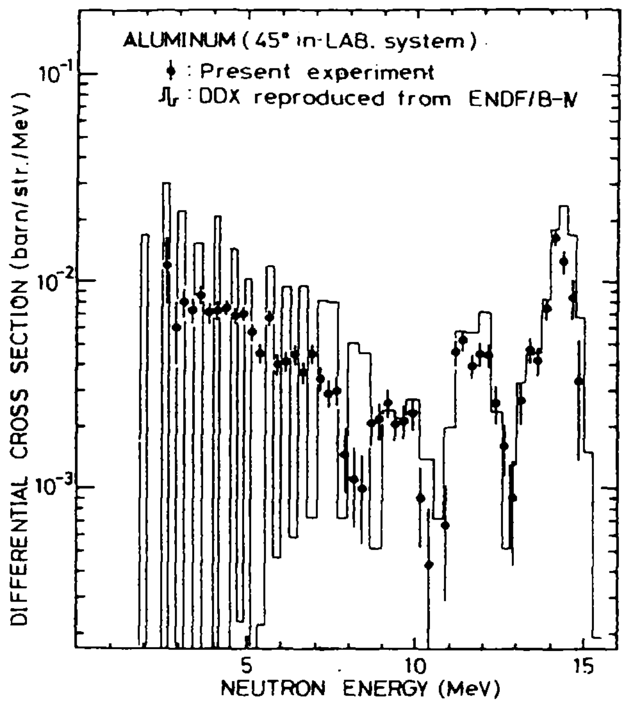

Fig.6 : DDX for aluminum at 45 deg.

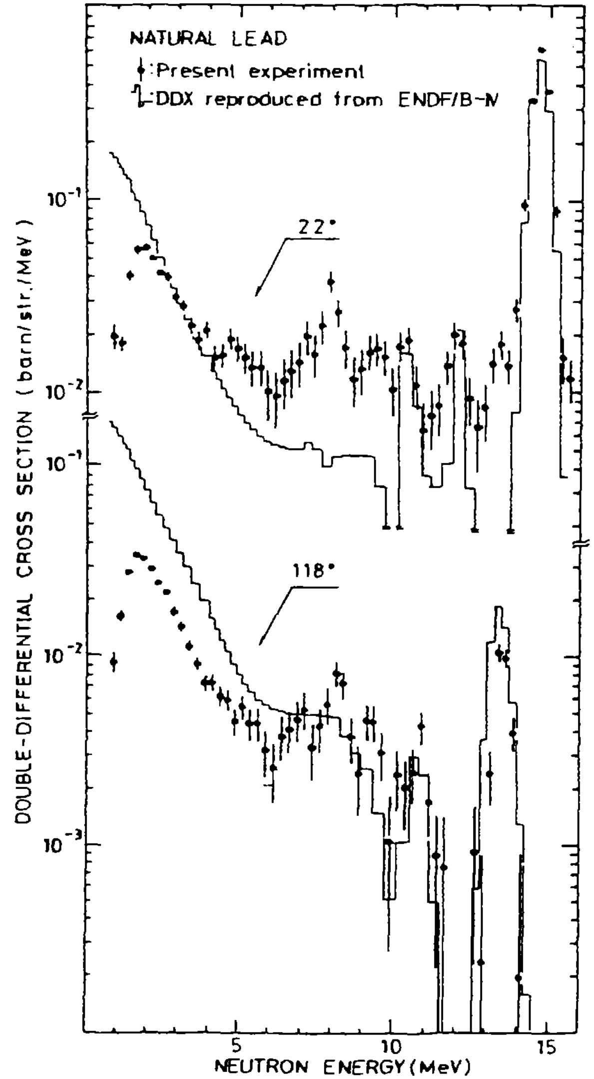

Fig. 7 : DDX for natural lead for 22 & 118°

VII. RIKKYO (ST. PAUL'S) UNIVERSITY

Department of Physics

VII-1 EFR-DWBA Analysis of the (n,d) and (n,t) Reaction Data on ^{6}Li at 14 MeV

K. Shibata, S. Shirato and H. Yamada

The experimental data reported in the Progress Report 1980[1] as well as the Zagreb data[2,3,4] on the reactions ^{6}Li(n, d)^{5}He and ^{6}Li(n,t)^{4}He at 14 MeV are compared with the exact-finite-range (EFR) distorted-wave-Born-approximation (DWBA) calculations using the computer codes DWUCK5[5] and DWBA4[6].

The optical-model potential parameters used in the DWBA calculations are given in Table I. The neutron potential parameters obtained by Hyakutake et al.[7], Set Li6-1 in Table I, were adopted for the entrance channel in the most calculations. As a result of the automatic parameter search through the code ELIESE-3[8], it was found that the elastic scattering data of Hyakutake et al. could be also well reproduced by Set Li6-2 in Table I. This parameter set was employed for the calculations of the two-step and knock-on processes using the code DWBA4 which is available at present without the spin-orbit coupling.

The results of our EFR-DWBA calculations are shown in Fig. 1 for the (n,d) case and Fig. 2 for the (n,t) case. The EFR-DWBA calculation reproduces very well the magnitude of the absolute cross section. In Fig. 1 the spectroscopic factor of 0.91 (1.07 for Set Li6-2) has been applied to the EFR-DWBA curve of $1p_{3/2}$ proton pickup, and also 0.93 has been done for $1p_{1/2}$ proton pickup. The EFR-DWBA calculation for knock-on did not give a better reproduction of the (n,d) angular distribution than that of proton pickup. The incoherent sum of the proton-pickup term with the spectroscopic factor of 0.82 and the ^{4}He pickup term is shown by the dotted line in Fig. 1.

Regarding the triton optical potential parameters, Set He4-1 in Table I obtained by Rosario-Garcia and Benenson[9] at 6.77 MeV gave the best fit to the $^{6}Li(n,t)^{4}He$ data even at 14 MeV in the deuteron pickup case, as shown in Fig. 2. Considering the deuteron pickup process alone, the value of the spectroscopic factor $S_{d\alpha}^{6Li}(2s)S_{nd}^{t}(1s)$ is obtained to be 0.94. The incoherent sum of the deuteron pickup, ^{3}He pickup and two-step terms with the factors applied to the EFR-DWBA curves of 0.64, 0.46 and 0.92, respectively, is given by the dotted line in Fig. 2. Assuming $S_{nd}^{t}(1s) = 1.5$, $S_{n^3He}^{\alpha}(1s) = 2.0$ and $S_{n\alpha}^{5He}(1p) = S_{np}^{d}(1s) = 1.0$, we obtain $S_{d\alpha}^{6Li}(2s) = 0.43$, $S_{t^3He}^{6Li}(2s) = 0.23$ and $S_{p^5He}^{6Li}(1p) = 0.82$.

References:

1) S. Higuchi, K. Shibata, M. Saito and S. Shirato, Progress Report 1980, JAERI, NEANDC(J)-67/U, INDC(JAP)-54/U, p. 64

2) V. Valković, G. Paić, I. Slaus, P. Tomas, M. Cerineo and G. R. Satchler, Phys. Rev. 139 (1965) B331

3) V. Valković, I. Slaus, P. Tomas and M. Cerineo, Nucl. Phys. A98 (1967) 305

4) D. Rendić et al., Rossendorf Reports 2 (1967) 143

5) P. D. Kunz, University of Colorado Report, unpublished

6) H. Yoshida, University of Tokyo, INS Report, unpublished

7) M. Hyakutake, M. Sonoda, A. Katase, Y. Wakuta, M. Matoba, H. Tawara and I. Fujita, J. Nucl. Sci. Technol. 11 (1974) 407

8) S. Igarasi, JAERI Report 1224,

9) E. Rosario-Garcia and R. E. Benenson, Nucl. Phys. A275 (1977) 453

Table I. Optical-model potential parameters used in the EFR-DWBA calculations.

The potential form is given by the following expression:

$$U(r) = U_C(r) - V/(1 + f_V(r)) - i\{W_V/(1 + f_W(r)) + W_G/f_G(r) + 4W_S f_W(r)/(1 + f_W(r))^2\} - \left(\frac{\hbar}{m_\pi c}\right)^2 V_{SO} \frac{1}{ar} f_V(r)(1 + f_V(r))^{-2} \vec{L}\cdot\vec{S},$$

where $f_V(r) = \exp\{(r - r_0 A^{1/3})/a\}$,

$f_W(r) = \exp\{(r - r_0' A^{1/3})/b\}$,

and $f_G(r) = \exp\{(r - r_0' A^{1/3})^2/b^2\}$.

Set	V (MeV)	W_G (MeV)	W_V (MeV)	W_S (MeV)	V_{SO} (MeV)	r_0 (fm)	r_0' (fm)	r_C (fm)	a (fm)	b (fm)	Ref
	Neutron optical potentials for ^{6}Li										
Li6-1	37.3	19.2	0.0	0.0	15.6	1.63	1.43	0.0	0.53	0.55	7)
Li6-2	62.48	8.2	0.0	0.0	0.0	0.97	1.50	0.0	0.79	1.09	
	Deuteron optical potentials for ^{5}He										
He5-1	115.0	0.0	0.0	0.675	0.0	1.26	1.80	1.4	0.73	0.31	
He5-2	118.0	6.3	0.0	0.0	5.8	0.89	1.77	1.3	0.91	1.39	*)
	Triton optical potentials for ^{4}He										
He4-1	145.0	0.0	2.0	0.0	4.0	0.85	2.00	1.4	0.70	0.65	9)

*) D. Miljanić and V. Valković, Nucl. Phys. A176 (1971) 110.

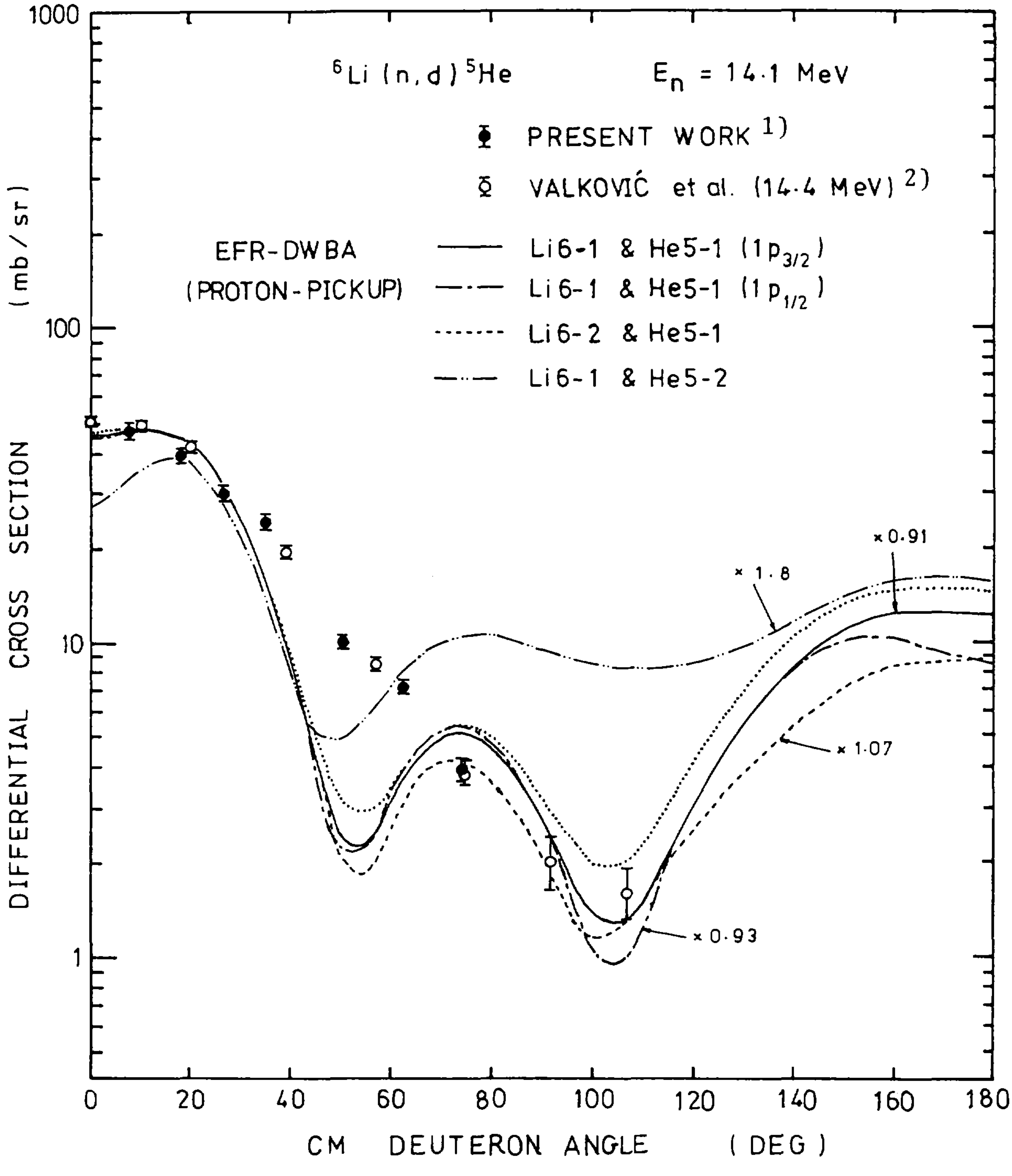

Fig. 1. EFR-DWBA predictions for the ^{6}Li(n,d)^{5}He reaction. The dotted curve is the incoherent sum of the $1p_{1/2}$ proton pickup term and the ^{4}He pickup one.

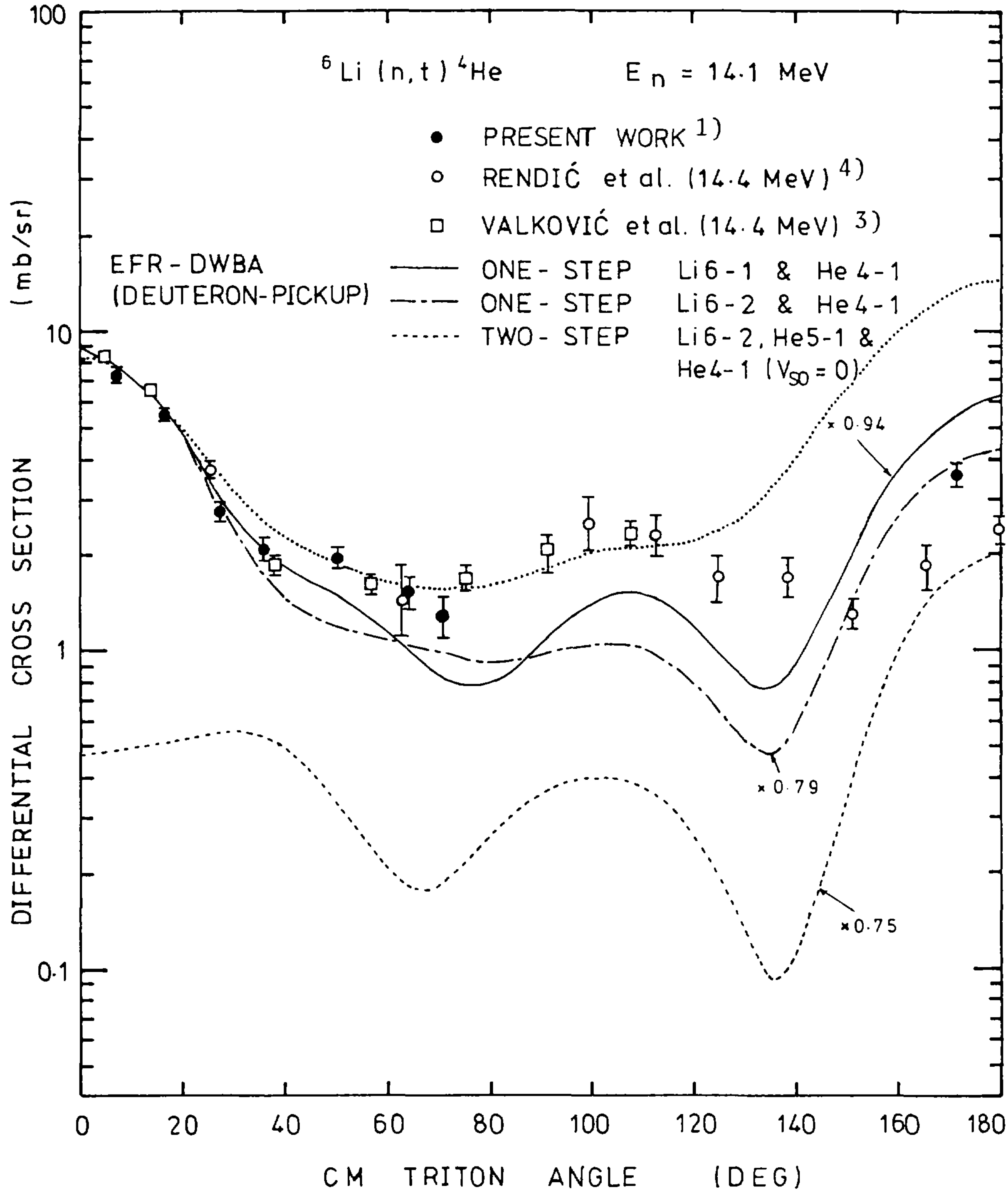

Fig. 2. EFR-DWBA predictions for the $^{6}Li(n,t)^{4}He$ reaction. The dotted curve is the incoherent sum of three terms of deuteron pickup, ^{3}He pickup and two-step process.

VIII. TOHOKU UNIVERSITY

Department of Nuclear Engineering

VIII-1 Measurement of double differential cross sections for (n,xn') reaction on C, Al, Ti and Mo at 15.2 MeV.

S. Iwasaki, T. Tamura, H. Suwa, H. Uchida
H. Arikawa*, H. Takahashi, and K. Sugiyama

The double differential cross sections (DDX) for (n,xn') reaction on carbon, aluminum, titanium, and molybdenum at 15.2 MeV have been measured in the second experiment of the DDX measurement program for the materials of fusion application at Fast Neutron Laboratory (FNL) of Tohoku University. Experimental conditions, apparatus and technique were almost same as the first experiment[1] with the exception of the points described in ref. [2]. Preliminally results of the experiment are as follows.

Carbon

Angular distribution of elastic and the first inelastic (Q=-4.43MeV) peaks which are well separated from each other and higher inelastic components are compared with recent experimental data by Glasgow et al.[3] at 14.93 MeV and the values taken from the ENDF/B-IV file. Present experimental results are consistent with those by Glasgow et al. Inelastic scattering cross sections for the higher excited states (Q=7.6MeV) and conmtinuum component are smaller than those by Hermsdorf et al.[4] at 14.6 MeV by a factor of about 1.5.

Aluminum

Elastic scattering peak have not been resolved from inelastic scattering component, because the energy spread of the source neutrons was large and the energy resolution of the spectrometer was not so good, too. General trend of the continuum secondary neutron spectrum are consistent with those by Hermsdorf et al.

---

* Present Address: Mitsubishi Atomic Power Industries, Ltd.

and the evaluation (ENDF/B-IV), but at several angles, the absolute values of the cross section are smaller than those of Hermsdorf et al. Angular distribution of the secondary neutron show forward peaking, and are well reproduced by the theoretical calculation by Akkermans et al.[5].

Titanium

The evaluated value (ENDF/B-IV) has unnatural discontinuity at 3.5 MeV in the spectrum, and the lower energy component which corresponds to the neutron groups from (n,2n) reaction gives an overestimated value comparing with the present experimental results. Angular distributions of the continuum component of the secondary neutrons also indicate the forward peaking distributions which are discrepant to the assumption of the isotropic distribution made in the evaluation.

Molybdenum

Angular spectra of secondary neutrons at forward angles show large cross sections in the continuum inelastic scattering and not consistent with the values of the ENDF/B-IV. The experiment for this sample has not been completed and is now in progress.

References:

1) S. Iwasaki et al., Proc. Int. Nat. Conf. on Nucl. Cross Sections for Technology, p73 Knoxville (1979).

2) S. Iwasaki et al., Ann. Report of FNL 1979/80, Tohoku Univ. (Jul. 1981).

3) D. W. Glasgow et al., Nucl. Sci. Eng., 61 521 (1976)

4) D. Hermsdorf et al., ZfK-277(Ü), Dresden, (1975)

5) J. M. Akkermans and H. Gruppelaar, Phys. Rev., C22, 73 (1980)

VIII-2 Measurement of prompt fission spectrum for ^{232}Th at 1.6 MeV

T. Tamura, S. Iwasaki, H. Suwa, H. Uchida

H. Arikawa*, H. Takahashi, and K. Sugiyama

Prompt fission neutron spectrum for ^{232}Th has been measured using the 4.5 MV Dynamitron accelerator at Fast Neutron Laboratory (FNL), TOF method and ring geometry[1]. Pulsed neutrons of 2-nsec width were produced by the T(p,n) reaction, and its energy was 1.6 MeV at the sample position. The sample was arranged as ring shape with sixteen plates of metal thorium** of each having a dimension of 5 x 5 x 0.3 cm^3, and placed at 45 degrees with respect to the proton beam. For estimating the background, lead sample was also used. Shadow bar which was fabricated with paraffine filled into a thin iron container was placed between the neutron source and neutron detector, and decrease the intensity of the source neutrons at the neutron detector by a factor of 2 x 10^{-5}, experimentally. A NE213 liquid scintillator was used as the neutron detector, which was encapsulated in the glass cell. It has high performance of the neutron-gamma discrimination, and high resolution[2]. Relative efficiency of the neutron detector has been obtained by observing angular distribution of the D(d,n) reaction cross section, and also using the calculated values by the O5S code[3]. Experimental electronics has been modefied a little from one used in the ordinary TOF spectrometer to obtain clear prompt gamma peaks (sample, and target gamma rays) in the time-of-flight spectrum in spite of applying the n-γ discrimination[1].

Since the drift of the time axis through the experimental run has been observed at preliminally measurement, the counting period of each run has been limited for 3 hours. There have been twelve runs for thorium sample, four runs for lead sample

---

* Present Address: Mitsubishi Atomic Power Industries, Ltd.

** borrowed from Kyoto University Reactor Institute and four runs for sample-out. The obtained spectra have been added together adjusting the gamma peak positions of each spectrum. The measured spectrum has been corrected for background by using a method of intercomparison with the elastic peaks of thorium and lead sample spectra. The corrections for detector efficiency, attenuation and multiple scattering have also been made. In the present study, the prompt fission neutron was assumed to have a Maxwell distribution. The least squares fitting method has been used to derive the Maxwellian temperature from the corrected spectrum. In this process, the measured values were weighted according to its covariance matrix which have been obtained considering the correlation between the experimental data along the energy axis. The derived Maxwellian temperature was 1.37 ± 0.05 MeV. This value is 8 % larger than the value of ENDF/B-IV and other estimated values[4,5], beyond the estimated uncertainty, as shown in Fig. 1. However, this value is consistent with the preliminally experimental result of 1.37 ± 0.01 MeV at 1.5 MeV as reported in NEANDC(J)-67/U, p69.

References:

1) T. Tamura et al., Ann. Report of FNL, Tohoku Univ. (Jul. 1981)

2) S. Iwasaki, H. Uchida, and K. Sugiyama, ibid.

3) R. E. Texter et al., ORNL-4160 (1968)

4) Y. S. Zamyatnin et al., At. Energ., 4 (1958) 443

Y. S. Vasil'ev et al. "Phys. Nucl. Fission", edited by N. A. Perfilov et al.(translated), Jerusalem (1964)

5) R. Batchelor et al., Nucl. Phys. 65 (1965) 236

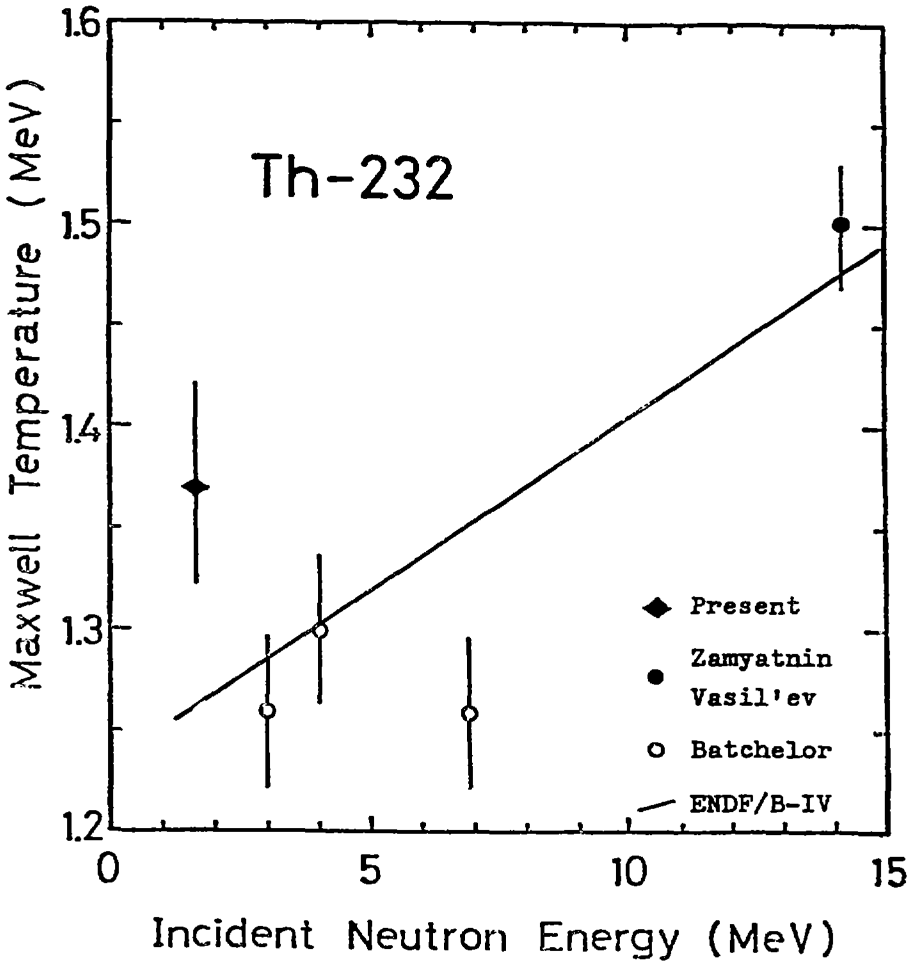

Fig. 1 Maxwell Temperature of ^{232}Th

T_m vs. E_n

VIII-3 MEASUREMENTS OF NEUTRON TOTAL CROSS SECTIONS FOR ^{232}Th[1)]

T.Iwasaki, M.Baba, K.Hattori, K.Kanda, S.Kamata and N.Hirakawa

Neutron total cross sections of ^{232}Th were measured from 0.05 to 10MeV with TOF method through the transmission experiment. White neutron sources with thick lithium target were used for 0.6 - 10MeV(by Li(d,n) reaction) and for 0.05 - 0.3MeV (by Li(p,n) reaction),respectively. For 0.3 - 0.6MeV, mono-energetic neutron source with thin LiF target was used.

Metallic thorium plates of 5.08cm x 5.08cm x 0.31cm were stacked in a stainless steel can and used as the transmission sample. The number of plates were varied according to the energy range of the measurement so that the transmission rate might be around 50%.

The neutron detector was NE213 organic scintillator of 5" ϕ x 2" thick coupled to XP2041 photomultiplier tube and ORTEC 269 base. TOF unit was composed of a time to amplitude converter and a 4000 channel pulse height analizer. n- discrimination with zero cross over method was employed. The detector bias was set to 0.2MeV for MeV region measurement and 0.02 KeV for the KeV region measurement. Ovreall time resolution was 3ns. The measurement for a graphite sample was made as well as the thorium sample and sample out run.

To obtain the cross sections the following corrections were considered to the measured data. 1) back ground correction, 2) the dead time correction for the PHA and 3) the correction for the self-shielding effect. The dead time of TAC and the effect of inscattering were insignificant.

The present data show good agreement with those of Foster[2] above 2.5MeV and with those of Whalen et.al.[3] from 0.1 to 5MeV. They differ more than 10% from the evaluation of ENDF/B4. From the measurement of cross section of carbon, the experimental uncertainty including systimatic errors was estimated to be less than ±2% for the whole energy range considered.

References:

1) T.Iwasaki, et.al., NETU37(1980) Tohoku University

2) D.G.Foster, et.al., Nucl.Instr.Method, 36 (1965) 1

3) J.F.Whalen, et.al., Nucl.Sci.& Eng. 67 (1978) 129

VIII-4

Neutron Scattering from ^{232}Th at 0.55, 2.4 and 5.7MeV

T. Iwasaki, M. Baba, K. Hattori, K. Kanda, S. Chiba, K. Kanoda and N. Hirakawa

In this study, secondary neutron energy spectra have been measured with TOF method for incident neutron energies of 0.55, 2.4 and 5.7MeV to obtain following informations,

1) Differential elastic scattering cross section (0.55MeV) or differential elastic group (including first 2^+ and second 4^+ state) cross sections (2.4 and 5.7MeV)
2) Inelastic scattering cross sections,
3) Evaporating temperature for continuum inelastic scattering

Experiment was performed by use of Tohoku University Dynamitron accelerator for generation of mono-energy neutrons via p-Li(0.55MeV), p-T (2.4MeV) and d-D (5.7MeV) reactions. The absolute values of cross sections were determined by normalizing to the sacttering cross sections of Hydrogen(2.4 and 5.7MeV) and Carbon(0.55MeV).

Present result for differential cross sections were in good agreement with those by Smith[1](0.55MeV) and Haouat[2](2.4MeV). The inelastic scattering cross sections obtained were closer to the values by ANL evaluation[3] than JENDL-2[4]. The evaporation temperature for continuum inelastic neutrons show agreement with other experimental values.

References;

1)A.B.Smith, Phys.Rev.,126,718 (1962)

2)G.Haouat et al.,NEANDC(E) 180"L"

3)J.Meadows et al., ANL/NDM-35 (1978)

4)T.Ohsawa and M.Ohta, J.Nucl.Tech.,18,408 (1981)

IX. Tokyo Institute of Technology

A. Department of Applied Physics

IX-A-1

Atomic mass difference between ^{135}Ce and ^{135}La

T. Saito*, T. Toriyama, M. Kanbe and K. Hisatake

A paper on this subject was published in Phys. Rev. C23 (1981) 1713.

Electron capture decay of ^{135}Ce(17.6 h) has been used to determine the mass difference between ^{135}Ce and ^{135}La. The main component of the positrons (0.36%/decay) was found to feed the 300 keV level in ^{135}La with triple coincidences between two annihilation radiations and γ rays. The end-point energy of the β^+ main component was determined to be 694 ± 13 keV. Thus the mass difference between ^{135}Ce and ^{135}La is determined to be 2016 ± 13 keV. No anomaly is found for the EC/β^+ ratio.

---

* Present address: Shimizu Construction Company Ltd.

B. Research Laboratory for Nuclear Reactors

IX-B-1

Gamma-rays from Resonance Neutron Capture in ^{56}Fe

H. Komano, M. Igashira, S. Katsuta and N. Yamamuro

Experiments were performed at the neutron energies of 5-80 keV, using a time-of-flight-technique. Pulsed neutrons were produced with a proton burst of 2ns from the T.I.T. pulsed 3-MV Pelletron accelerator, incident on a thin lithium film at the repetition rate of 2MHz. The target was a $6 \times 6 \times 1.9$ cm plate of natural iron placed at a flight path of 41 cm from the neutron source. The gamma-ray detector was a 60-cc coaxial high purity Ge detector, which was shielded against background gamma-rays and neutrons by lead and borated paraffin. The distance between the target and the detector was 11 cm. The detector made an angle of 90° with respect to the proton beam direction. The gamma-ray detection efficiency was measured using calibrated standard gamma-ray sources and gamma-rays from the $^{27}Al(p,\gamma)^{28}Si$ resonance reaction at 2046 keV. The neutron flux was measured with a 1-mm thick ^{6}Li glass scintillation detector, which was placed between the neutron source and the target.

As a result, four partial radiation widths were obtained for gamma-ray transitions from three resonance states in ^{56}Fe. The correction for multiple scattering and self shielding was made for a s-wave resonance capture. The results are shown in Table 1 and 2, in comparison with other ones. Our results are in good agreement with the results of Jackson et al.[1], but there is a little discrepancy between our results and those of Beer et al.[2]. The theoretical value in Table 1. was calculated with a valence capture model, and it explains about a half of our experimental value.

References:

1) H.E. Jackson et al., Phys. Rev. C4 (1971) 1314.

2) H. Beer et al., Z. Physik A284 (1978) 173.

Table 1. The partial radiation widths for s-wave resonance

E_n (keV)	Γ_γ (eV)	E_f (MeV)	J_f^π	$\Gamma_{\gamma p}$ (eV) experimental present	others (a)	others (b)	theoretical valence model
27.68	1.44	0	$1/2^-$	0.117 ± 0.018	0.145 ± 0.023	0.112	0.0605
		0.014	$3/2^-$	0.076 ± 0.013	0.035 ± 0.013		

(a): ref.2 (b): ref.1

Table 2. The partial radiation widths for p-wave resonances

E_n (keV)	J_i^π	E_f (MeV)	J_f^π	$g \frac{\Gamma_n \Gamma_{\gamma p}}{\Gamma}$ (eV) present	others (a)	others (b)
34.25	$1/2^-$	0	$1/2^-$	0.204 ± 0.031	0.301 ± 0.067	0.180
38.38		0.014	$3/2^-$	0.080 ± 0.014	0.146 ± 0.035	

(a): ref.2 (b): ref.1

IX-B-2

Gamma-Ray Spectrum from Capture of 400 keV Neutrons in Sn

M. Igashira, T. Maruyama*, H. Kitazawa and N. Yamamuro

A capture gamma-ray spectrum in Sn has been measured at the neutron energy of 400 keV. The T.I.T. pulsed 3-MV Pelletron accelerator provided proton bursts of 2-ns width at 2-MHz repetition rate, and neutrons were produced by the $^{7}Li(p,n)^{7}Be$ reaction. A 7.5 cm$\phi \times$ 15 cm NaI(Tl)-detector centered in an annular NaI(Tl)-crystal, which was surrounded by a heavy shield consisting of paraffin, boric acid, and lead, was used as a gamma-ray detector. The detection efficiency and the response functions were determined with gamma-rays from calibrated radioactive sources and $^{27}Al(p,\gamma)^{28}Si$, $^{9}Be(p,\gamma)^{10}B$, and $^{19}F(p,\alpha\gamma)^{16}O$ reactions. The sample was a 4.5 cm$\phi \times$ 4.5 cm natural tin located at 15 cm from the neutron source. The distance between the sample and the NaI(Tl)-detector was 113 cm. The detector axis made an angle of 125° with respect to the proton beam direction.

The capture gamma-ray spectrum, shown in Fig. 1, was obtained after background subtraction, spectrum unfolding, and correction for gamma-ray self-absorption and scattering in the sample. A histogram is the spectrum calculated by the computer code CASTHY[1)] based on a statistical model. A comparison between two spectra shows that two peaks observed at 5.5 MeV and at 6.5 MeV and a dip at 2 MeV could not be explained by the statistical model.

Reference:

1) S. Igarashi, J. Nucl. Sci. Technol. 12, 67 (1975)

---

* Mitsubishi Electric, Ltd.

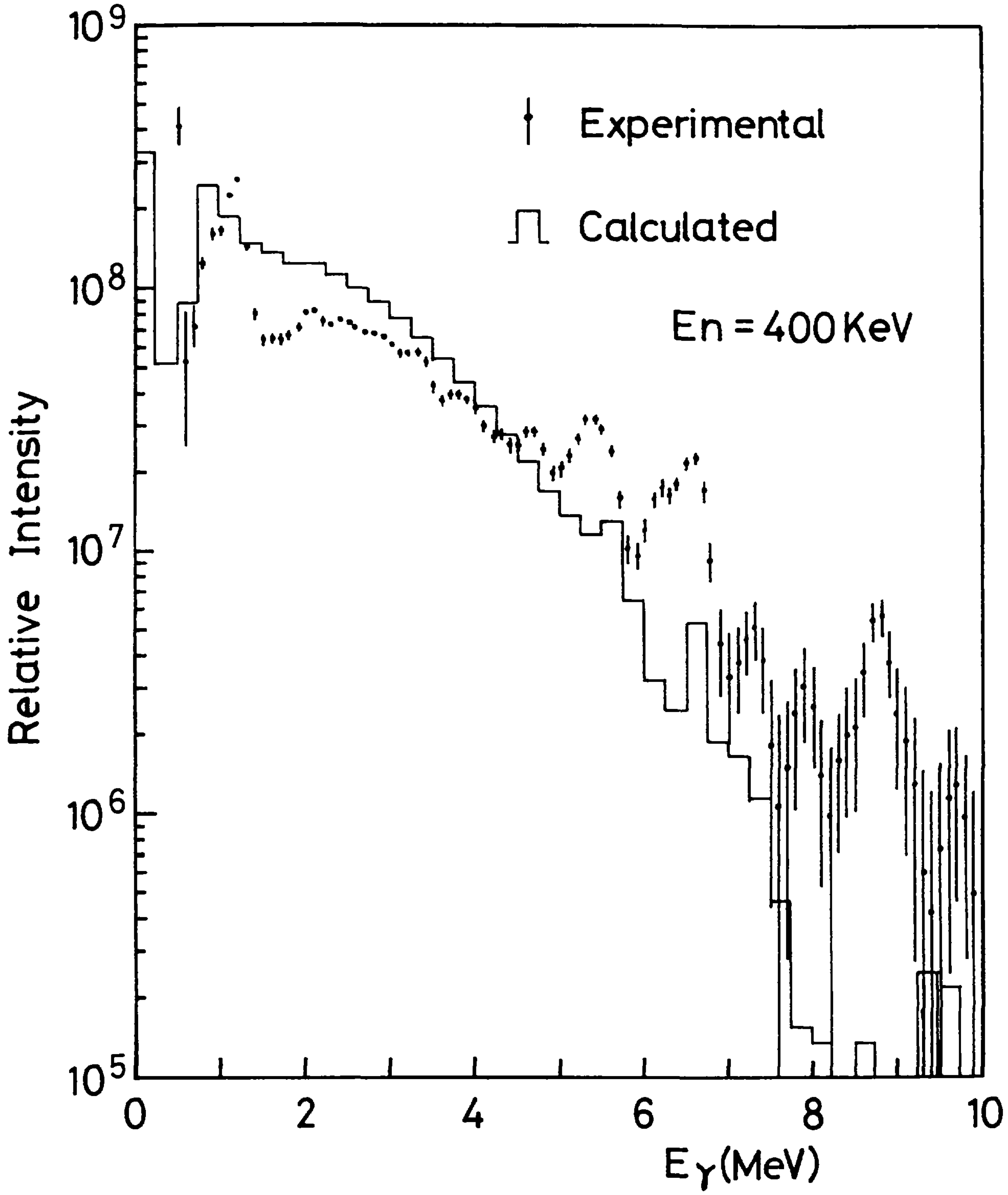

Fig.1 Sn(n, γ) γ-ray spectrum

IX-B-3

Neutron Capture Gamma-ray Spectrum for ^{133}Cs

H. Shirayanagi*, T. Yoshinari, M. Igashira and N. Yamamuro

The Monte-Carlo program RESPO-M1 for the calculation of the gamma-ray response function of the liquid scintillation counter has been improved in the process of electron slowing-down. The slowing-down of scattered electron and electron-positron pair in the scintillator was treated by Condensed Case History method[1]. The results of calculation were compared with the measured gamma-ray spectra, from 0.662 MeV (^{137}Cs) to 6.13 MeV (^{16}N), and the energy resolution of detector was determined.

Gamma-rays emitted from the (n,γ) reactions of ^{133}Cs, ^{181}Ta and ^{197}Au were detected by a couple of C_6D_6 liquid scintillation counters. The energy of neutrons was from 1.5 to 75 keV, which was determined by the time-of-flight method. The measured spectra were unfolded with the improved RESPO-M1 code, and the spectra result in the good agreement with the previous ones for ^{181}Ta and ^{197}Au[2]. The spectrum for ^{133}Cs, multiplied by the gamma-ray energy and normalized per neutron capture, is shown in Fig. 1. For comparison, the result of Bergqvist and Starfelt[3] is represented by sold line. Both data differ in the relative intensity between the higher energy region and the lower energy region.

References:

1) M.J. Berger, " Monte-Carlo Calculation of the Penetration and Diffusion of Fast Charged Particles " Methods in Computational Physics, vol. 1, p.135 (1963).

2) H. Shirayanagi et al., Progress Report NEANDC(J)-67/U, p.70 (1980).

3) I. Bergqvist and N. Starfelt, Nucl. Phys. 39, 529 (1962).

---

* The Tokyo Electric Power Co., Inc.

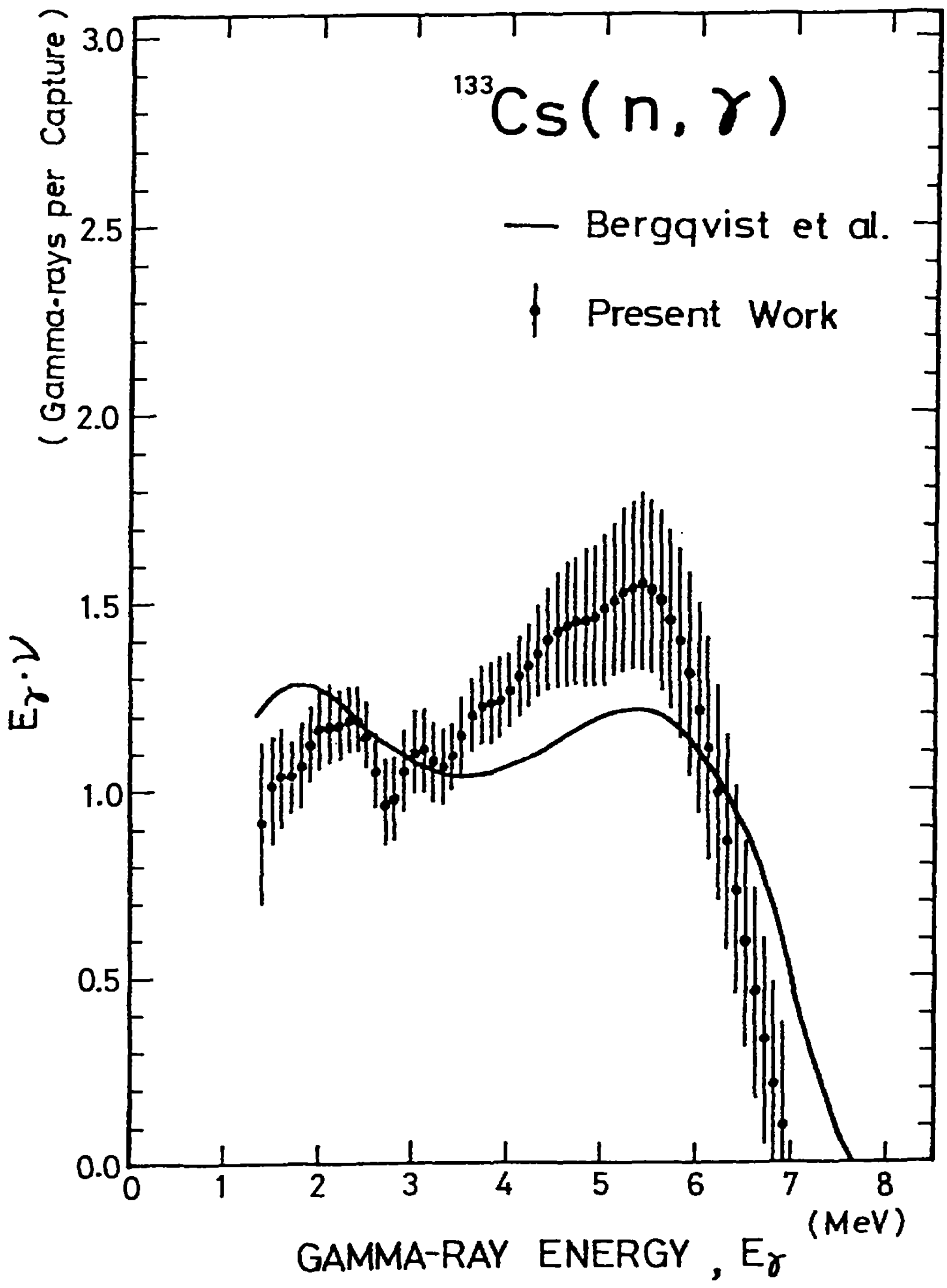

Fig. 1 Gamma-rays from ^{133}Cs(n,γ) reaction.

IX-B-4

Neutron Capture Cross Section Measurements of Nb-93, I-127, Ho-165, Ta-181 and U-238 between 3.2 and 80 keV+

N. Yamamuro, K. Saito*, T. Emoto**, T. Wada***,

Y. Fujita**** and K. Kobayashi****

The neutron capture cross sections of ^{93}Nb, ^{127}I, ^{165}Ho, ^{181}Ta and ^{238}U were measured from 3.2 to 80 keV using the time-of-flight method. The neutron beam was produced by the KURRI 46-MeV linear accelerator and capture γ-rays were detected by a C_6F_6 or C_6D_6 liquid scintillation detector. As the result of the use of a direct-coupled operational preamplifier, the detector recovered rapidly from the γ-flash such that data for higher energy neutrons can be obtained in spite of the short flight path of 11.7 m. The neutron sensitivities of both detectors are compared and the superiority of the C_6D_6 detector is shown.

The experimental results of capture cross sections, corrected for resonance self-shielding and multiple scattering and normalized to the 24-keV absolute values, are shown numerically and graphically, and compared with other data. The agreement between the data is fairly good for ^{165}Ho and ^{238}U, but not for ^{93}Nb, ^{127}I and ^{181}Ta. The discrepancy between the data may be caused by the difference of the reference cross sections used for each experiment.

---

* Japan Atomic Energy Research Institute.

** University of Illinois, USA.

*** Institute of Space and Aeronautical Science, University of Tokyo.

**** Research Reactor Institute, Kyoto University.

+ This paper was published in the Journal of Nuclear Science and Technology, 17[8], pp.582~592 (August 1980).